

Spin current and internal Zeeman field in spin-orbit coupled ringsHsiu-Chuan Hsu^{1,2,*} and Tsung-Wei Chen^{3,†}¹*Graduate Institute of Applied Physics, National Chengchi University, Taipei 11605, Taiwan*²*Department of Computer Science, National Chengchi University, Taipei 11605, Taiwan*³*Department of Physics, National Sun Yat-sen University, Kaohsiung 80424, Taiwan* (Received 14 January 2023; revised 20 February 2023; accepted 8 March 2023; published 24 March 2023)

We investigate the one-dimensional quantum ring constructed by the spin-orbit coupled material, in which the quantum spin-Hall Bernevig-Zhang (BZ) Hamiltonian and Rashba-Dirac (RD) type spin-orbit coupling are taken into account (called RD-BZ Hamiltonian in this paper). It is known that the curvature of the ring generates an out-of-plane effective magnetic field, acting as an internal Zeeman field. We find that only the BZ coupling can change the strength of the internal Zeeman field, which enables us to detect the effect of the internal Zeeman field. Furthermore, we find that the total angular momentum is conserved in the RD-BZ Hamiltonian, and the energy eigenvalue and wave function must be modified to fit the conserved quantity, which are ignored in the previous studies. The conductance without leads is discussed. Different from the previous results, we find that the conductance behaves like a beat phenomenon resulting from the interplay between the magnetic flux and Aharonov-Casher (AC) phase, and thus, it can oscillate without passing through the insulating state in some regimes of magnetic flux or AC phase. Importantly, we find that the conductance with integer and half-integer magnetic flux provides us a method to measure the AC phase. The cancellation of the internal Zeeman field due to the BZ coupling can be detected by using specific fractional magnetic flux. In the ring with nonvanishing RD and BZ couplings, the conductance can exhibit a quasiplateau near the small RD coupling. The increase in the strength of BZ coupling would result in wider quasiplateau in conductance, which implies that the ring could remain insulating state (or conducting state) regardless of the small change in RD coupling. The thermal average of spin and charge currents are calculated at low temperatures without impurities. Importantly, we find that the persistent spin and charge currents as a function of the magnetic flux exhibit nodelike lines, which amazingly are perpendicular to each other. As a consequence, the persistent spin current could be nonzero even when the charge current vanishes at nonzero magnetic flux. The result suggests a pure spin current in quantum rings, and its direction can be reversed by changing the magnetic flux. The increase in the BZ coupling would exhibit the plateaulike pure spin current.

DOI: [10.1103/PhysRevB.107.125419](https://doi.org/10.1103/PhysRevB.107.125419)**I. INTRODUCTION**

Berry proposed a pioneering result that the cyclic and adiabatic evolution of quantum states acquires a phase with geometric nature [1]. This geometric phase depends only on the geometry of the path traveled by the quantum state in the parameter space, which was observed in various experiments [2]. The geometric phase governed by the topology of the quantum state opens up a new field in the quantum transport [3]. The interplay between the quantum geometric phase with the spatial shape of nanostructures has been utilized for exotic electronics [4]. On the other hand, broken symmetry in semiconductor gives rise to various intrinsic spin-orbit interaction (SOI). Two typical examples are Dresselhaus SOI induced by bulk inversion symmetry [5] and the Rashba SOI induced by structure inversion symmetry [6]. As a result, the transport affected by the spin-orbit interaction in semiconductor heterostructure plays the central part in growing

studies of spintronics [7,8] and facilitates the integration of quantum computer [9]. Moreover, many investigations have strongly boosted by the study of the Rashba SOI in low dimensional systems [10], including magnetoconductance oscillations [11,12] and persistent charge current [13,14], and the effect of strong light-matter coupling was recently investigated [15]. The transport phenomenon in mesoscopic rings with SOI was studied experimentally [16]. The persistent current was also extensively investigated within the quantum ring [17–20] and observed [21].

One of the important features of quantum rings is quantum interference which can be caused by the two typical phases: Aharonov-Bohm (AB) [22] and Aharonov-Casher (AC) effects [23]. The quantum interference has been demonstrated experimentally [24]. The theoretical study relies on constructing an effective model Hamiltonian. Nitta *et al.* proposed a spin-interference device with Rashba spin-orbit interaction and the resulting conductance can be modulated by the AC phase [25]. This proposed structure is a one-dimensional ring, but the Hamiltonian is non-Hermitian. The procedure for constructing correct one-dimensional Hamiltonian of a quantum ring from two-dimensional Hamiltonian has been

*hcjhsu@nccu.edu.tw

†twchen@mail.nsysu.edu.tw

proposed by Meijer *et al.* [26], which corresponds to the quantization approach for nonrelativistic particles constrained to lower dimensions [27]. This procedure was also applied to the ring with various shapes [28], in which the topologically nontrivial spin textures were exhibited by deforming the shape of the ring. The transfer matrix method for calculating the conductance with leads was proposed in Ref. [29]. We also note that the spin current resulting from AB and AC effects in mesoscopic rings with both Rashba and Dresselhaus SOI was studied in Ref. [30], and the conductance in rings with heavy holes has been investigated in number of studies [31,32].

Another important feature of quantum rings is the curvature induced effective magnetic field on the ring, proposed by Ying *et al.* in Ref. [28]. In the absence of spin-orbit interaction, the curvature of the ring still provides an effective local field in the direction perpendicular to the plane of the ring, which is called the internal Zeeman field. However, the resulting energy splitting due to the internal Zeeman field is ambiguous in the absence of spin-orbit interaction. This is because the curvature of the ring also affects the orbital angular momentum of the particle on the ring, and thus, the energy splitting should take the total angular momentum into account. We also note that the conservation of angular momentum in the ring with leads was discussed in Ref. [12], but the correction to the internal Zeeman field was ignored. Therefore we need an effective system that can mimics the internal Zeeman field in the ring and investigate its influence to the conductance. An intriguing question arises: can we cancel the internal Zeeman field and detect the existence of the local field on the ring?

Moreover, the mechanism of spin-orbit coupling enable us to manipulate spin by using electric field. Quantum-spin Hall material shows the transport of spin at edges of sample with vanishing charge-Hall conductance in the absence of an external magnetic field [33]. Topological insulators in the strong regime of spin-orbit interaction exhibit the helical electron states at the surface of sample [34,35]. We also note that the quantum transport of two-dimensional Dirac electrons in a ring structure has been studied. [36]. It has been shown that the opposite geometric phase for two valleys leads to valley-polarized transport in a quantum ring. Recently, the quantum ring in contact with topological superconducting nanowire was investigated [37]. Interestingly, the quantum spin-Hall effect has a simple classical analog [33]. The charged particle has an orbital motion under the action of two-dimensional simple harmonic oscillator. The spin part of the charged particle couples to the orbital motion such that only z component of spin survives and the total angular momentum is conserved. In this regard, the ring constructed by the quantum spin-Hall materials can be a proper candidate to investigate the behavior of the internal Zeeman interaction and its influences to the spin current in the ring.

Motivated by these previous studies, we investigate the quantum ring in the presence of Bernevig-Zhang (BZ) [33] and Rashba-Dirac (RD) spin-orbit couplings. Interestingly, we find that the BZ coupling plays the role of an internal Zeeman field. The RD type coupling governs the tangential component of spin on the ring. Furthermore, because of the cylindrical symmetry, the resulting Hamiltonian also has a conserved total angular momentum. This leads to the mod-

ifications of the energy eigenvalue and eigenvectors, which were ignored in the previous works on quantum rings. The Zeeman interaction (coupling of spin and external magnetic field) is neglected in the present paper. In this regard, the phase acquired by the charged particle with spin can be divided into two part: pure electronic part (magnetic flux) and pure spin part [Aharonov-Casher (AC) phase]. The resulting conductance (without leads) then shows the beat phenomena and can oscillate without passing insulating state. Furthermore, the fractional quantized magnetic flux (or AC phase) can lead to the vanishing of oscillations in conductance. We also find that the internal Zeeman field can be controlled by the BZ coupling, which results in the increase of quasiplateau in conductance. The thermal average of spin and charged currents are calculated without the presence of impurities. The spin current vanishes when BZ coupling exactly cancels the internal Zeeman field. Furthermore, both the spin and charge currents exhibit nodelike lines which perpendicular to each other, and thus, pure spin current can be obtained in the quantum ring.

This paper is organized as follows. In Sec. II, the one-dimensional Hamiltonian for the ring with RD and BZ couplings is derived. The energy eigenvalues and eigenvectors are obtained by considering the quantum number from the conservation of total angular momentum. In Sec. III, the local spin orientation and internal Zeeman field are derived. The conductance is calculated and the effects of BZ coupling are discussed in Sec. IV. The thermal average of spin and charge currents are calculated and discussed in Sec. V. The conclusions are given in Sec. VI.

II. EFFECTIVE HAMILTONIAN

We study the Bernevig-Zhang (BZ) Hamiltonian including Rashba-Dirac (RD) type spin-orbit coupling, here-and-after called RD-BZ Hamiltonian in this paper. The two-dimensional Hamiltonian reads

$$H_{2D} = \frac{p_x^2 + p_y^2}{2m} + H_R + H_C + H_{BZ} + V(\mathbf{r}), \quad (1)$$

$V(\mathbf{r}) = \frac{1}{2}K(|\mathbf{r}| - R)^2$ is the confining potential, where R is the radius of the one-dimensional ring. The term H_R and H_C are Rashba [6] and Dirac-type Hamiltonians, respectively, and H_{BZ} is the BZ hamiltonian [33]. These Hamiltonians are written as

$$\begin{aligned} H_R &= \alpha(\sigma_x p_y - \sigma_y p_x), \\ H_C &= \eta(\sigma_x p_x + \sigma_y p_y), \\ H_{BZ} &= g_1(y p_x - x p_y)\sigma_z + g_2(x^2 + y^2). \end{aligned} \quad (2)$$

The Pauli spin matrices are denoted as σ_x , σ_y , σ_z . In the presence of external magnetic field, $\mathbf{B} = B\hat{z}$. The momentum in Eq. (1) is replaced by

$$\mathbf{p} \rightarrow \mathbf{\Pi} = \mathbf{p} - e\mathbf{A}, \quad (3)$$

where $e = -|e|$ for an electron, and the vector potential \mathbf{A} is given by

$$\mathbf{A} = (A_x, A_y, A_z) = \left(-\frac{1}{2}yB, \frac{1}{2}xB, 0\right). \quad (4)$$

Equation (1) is written as

$$H_{2D} = \frac{\Pi_x^2 + \Pi_y^2}{2m} + \alpha(\sigma_x \Pi_y - \sigma_y \Pi_x) + \eta(\sigma_x \Pi_x + \sigma_y \Pi_y) + g_1(y \Pi_x - x \Pi_y) \sigma_z + g_2(x^2 + y^2) + V(\mathbf{r}). \quad (5)$$

Consider the circular ring of radius R (constant curvature $1/R$), we define the azimuthal angle ϕ as $x = R \cos \phi$ and $y = R \sin \phi$, and the Pauli spin matrices in the planar coordinate are give by $\boldsymbol{\sigma} = \sigma_x \hat{e}_x + \sigma_y \hat{e}_y + \sigma_z \hat{e}_z = \sigma_r \hat{e}_r + \sigma_\phi \hat{e}_\phi + \sigma_z \hat{e}_z$. Use the coordinate transformations $\hat{e}_x = \cos \phi \hat{e}_r - \sin \phi \hat{e}_\phi$, and $\hat{e}_y = \sin \phi \hat{e}_r + \cos \phi \hat{e}_\phi$, we have

$$\begin{aligned} \sigma_r &= \sigma_x \cos \phi + \sigma_y \sin \phi, \\ \sigma_\phi &= -\sigma_x \sin \phi + \sigma_y \cos \phi. \end{aligned} \quad (6)$$

It can be shown that the commutation relations of σ_r , σ_ϕ and σ_z are given by

$$[\sigma_r, \sigma_\phi] = 2i\sigma_z, \quad [\sigma_z, \sigma_r] = 2i\sigma_\phi, \quad [\sigma_\phi, \sigma_z] = 2i\sigma_r. \quad (7)$$

Follow the procedure given in Ref. [26], where the strictly one-dimensional Hamiltonian is derived by averaging \hat{H}_{2D} with the ground-state radial wave function. Neglect the irrelevant additional constant terms (only shift the zero energy), the one-dimensional ring with RD-BZ spin-orbit interaction is replaced by $H_{2D} \rightarrow \hat{H}_0$, we have the following compact form (the derivation is given in Appendix A):

$$\hat{H}_0 = \epsilon \hat{D}_0^2, \quad \epsilon = \frac{\hbar^2}{2mR^2}, \quad (8)$$

where the operator \hat{D}_0 is given by

$$\hat{D}_0 = \frac{\hat{\ell}_z}{\hbar} + \gamma_0 + Z_\alpha \sigma_r + Z_\eta \sigma_\phi - b \sigma_z, \quad (9)$$

with the orbital angular momentum operator

$$\hat{\ell}_z = -i\hbar \frac{\partial}{\partial \phi}. \quad (10)$$

In the absence of Dirac and BZ coupling ($Z_\eta = 0$ and $b = 0$), Eq. (9) goes back to the pure Rashba result as shown in Ref. [29]. The coefficients γ_0 , Z_α , Z_η , and b are dimensionless quantities, which are given by

$$Z_\alpha = \frac{mR\alpha}{\hbar}, \quad Z_\eta = \frac{mR\eta}{\hbar}, \quad b = \frac{mR^2 g_1}{\hbar}, \quad (11)$$

where $\hbar = h/2\pi$ and h is the Planck constant. The symbol γ_0 is the magnetic flux denoted as

$$\gamma_0 = \frac{\Phi}{\Phi_0}, \quad (12)$$

where $\Phi = B\pi R^2$ is the magnetic flux through the ring and $\Phi_0 = h/|e|$ is the flux quantum. The energy eigenvalues and eigenvectors of Eq. (8) can be exactly solved, and we discuss this in the following sections.

A. Absence of RD-BZ coupling

In the absence of RD-BZ spin-orbit interaction, dimensionless parameters Z_α , Z_η , and b vanish, and the Hamiltonian

Eq. (8) reduces to

$$\hat{H}_0 = \epsilon \left(-i \frac{\partial}{\partial \phi} + \gamma_0 \right)^2. \quad (13)$$

The energy eigenvalue is then given by

$$E = \epsilon(\gamma_0 + n)^2 \quad (14)$$

with the corresponding eigenvectors

$$\psi(\phi) = \frac{1}{\sqrt{2\pi}} e^{in\phi}, \quad n = 0, \pm 1, \pm 2, \dots \quad (15)$$

The magnetic flux γ_0 can be eliminated by using the gauge transformation $\psi(\phi) \rightarrow \psi(\phi) e^{-i\gamma_0\phi}$. This means that the magnetic flux γ_0 in the eigenvalue is attributed to the phase acquired by the charged particle traveling a polar angle ϕ , which is the pure electronic behavior.

B. Presence of RD-BZ SOC

In the presence of RD-BZ spin-orbit interaction, we find that the operator \hat{D}_0 [Eq. (9)] commutes with the total angular momentum (see Appendix) $\hat{J}_z = \hat{\ell}_z + (\hbar/2)\sigma_z$, i.e.,

$$\left[\hat{\ell}_z + \frac{\hbar}{2}\sigma_z, \hat{D}_0 \right] = 0. \quad (16)$$

The energy eigenvectors of Eq. (8) should be characterized by using quantum numbers of \hat{J}_z . The eigenvector of \hat{J}_z can be written as $|n, \sigma\rangle$, where

$$\begin{aligned} |n, \uparrow\rangle &= e^{in\phi} |\uparrow\rangle, \quad \hat{J}_z |n, \uparrow\rangle = (n + \frac{1}{2})\hbar |n, \uparrow\rangle, \\ |n, \downarrow\rangle &= e^{in\phi} |\downarrow\rangle, \quad \hat{J}_z |n, \downarrow\rangle = (n - \frac{1}{2})\hbar |n, \downarrow\rangle, \end{aligned} \quad (17)$$

where

$$|\uparrow\rangle = \begin{pmatrix} 1 \\ 0 \end{pmatrix}, \quad |\downarrow\rangle = \begin{pmatrix} 0 \\ 1 \end{pmatrix} \quad (18)$$

are the eigenvectors of spin z-component σ_z . This implies that the trial energy eigenvector of \hat{H}_0 would be of the form

$$|\text{Trial}\rangle = \begin{pmatrix} \chi_1 e^{i(j_z - \frac{1}{2})\phi} \\ \chi_2 e^{i(j_z + \frac{1}{2})\phi} \end{pmatrix}, \quad (19)$$

where j_z is the eigenvalue of the total angular momentum $\hat{\ell}_z + \frac{\hbar}{2}\sigma_z$. It is easy to show that $|\text{Trial}\rangle$ is the eigenvector of the total angular momentum operator $\hat{J}_z = \hat{\ell}_z + (\hbar/2)\sigma_z$ with eigenvalue j_z , i.e.,

$$\hat{J}_z |\text{Trial}\rangle = j_z \hbar |\text{Trial}\rangle. \quad (20)$$

After straightforward algebraic calculations, the eigenvectors of the Hamiltonian (8) are given by (see Appendix)

$$\psi_\uparrow(\phi) = \frac{e^{ij_z\phi}}{\sqrt{2\pi}} \begin{pmatrix} \cos \frac{\xi}{2} e^{-i\phi/2} \\ \sin \frac{\xi}{2} e^{i\theta} e^{i\phi/2} \end{pmatrix} \quad (21)$$

and

$$\psi_\downarrow(\phi) = \frac{e^{ij_z\phi}}{\sqrt{2\pi}} \begin{pmatrix} -\sin \frac{\xi}{2} e^{-i\phi/2} \\ \cos \frac{\xi}{2} e^{i\theta} e^{i\phi/2} \end{pmatrix}, \quad (22)$$

where $\sigma = \uparrow$ represents the plus sign (lower energy), and $\sigma = \downarrow$ represents the minus sign (greater energy). The total

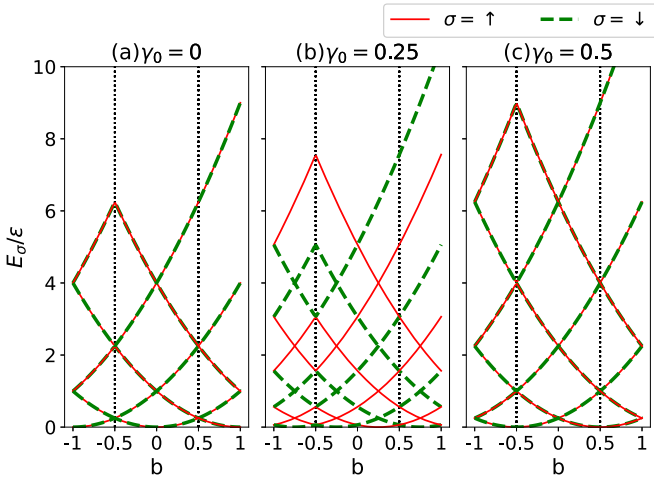


FIG. 1. The energy dispersion as a function of b , given by Eq. (27), with $Z = 0$ and $n = -2, -1, 0, 1, 2$. (a) $\gamma_0 = 0$, (b) $1/4$, and (c) $1/2$ and an additional band for $E_{-3\uparrow}$ is included to show the degeneracy between $(-3, \uparrow)$ and $(2, \downarrow)$.

angular momentum quantum number is

$$j_z^\sigma = n + \frac{1}{2}\sigma \quad (23)$$

and it will be further discussed below. The parameter ξ and θ are given by

$$\tan \theta = \frac{Z_\eta}{Z_\alpha}, \quad \tan \xi = -\frac{|Z|}{b + \frac{1}{2}}, \quad (24)$$

where

$$\begin{aligned} Z &= Z_\alpha + iZ_\eta \\ &= |Z|e^{i\theta}, \quad |Z| = \sqrt{Z_\alpha^2 + Z_\eta^2}. \end{aligned} \quad (25)$$

The coordinate ξ is the local spin tilt angle. In the present case, we have $\langle \psi_\uparrow(\phi) | \sigma_z | \psi_\uparrow(\phi) \rangle = +\cos \xi$ (called spin-up state) and $\langle \psi_\downarrow(\phi) | \sigma_z | \psi_\downarrow(\phi) \rangle = -\cos \xi$ (called spin-down state). We also note that

$$\tan \frac{\xi}{2} = \pm \frac{b + \frac{1}{2}}{|Z|} \pm \frac{1}{|Z|} \sqrt{|Z|^2 + \left(b + \frac{1}{2}\right)^2} \quad (26)$$

and the choice of eigenvectors [Eq. (21) and (22)] correspond to the minus sign in Eq. (26). The corresponding energy eigenvalues of Hamiltonian (8) are given by

$$E_{n\sigma} = \epsilon \left(\gamma_0 + j_z^\sigma - \sigma \sqrt{|Z|^2 + \left(b + \frac{1}{2}\right)^2} \right)^2, \quad (27)$$

The energy as a function of b for three values of γ_0 and $Z = 0$ is shown in Fig. 1. When $\gamma_0 = 0$ [Fig. 1(a)], the states with opposite j_z^σ are degenerate. When $\gamma_0 = 0.25$ [Fig. 1(b)], the degenerate bands split and extra band crossings appear at $b = -0.25, -0.75$. The degenerate pairs of quantum number at band crossings for spin up states are $(n, -n - 1)$, whereas for the spin down states are $(n, -n)$. When $\gamma_0 = 0.5$ [Fig. 1(c)], the states with $(n + 1, \uparrow)$ and $(-n, \downarrow)$ are degenerate. Although the spin up and down states are degenerate, their quantum number n differ by $2n + 1$.

The term j_z^σ in the wave function is the total angular momentum quantum number, which should be $j_z^\sigma = n + q_\sigma$ with $n = 0, \pm 1, \pm 2, \dots$ describing the rotation of electron in the sense of counterclockwise (“+” plus sign) or clockwise (“-” minus sign). In the absence of spin-orbit interaction, we should have

$$E_\uparrow = E_\downarrow = \epsilon(\gamma_0 + n)^2 \quad (28)$$

regardless of the sense of rotation. By using Eq. (27), we have $q_\uparrow - \frac{1}{2} = q_\downarrow + \frac{1}{2} = 0$, and this gives $q_\uparrow = \frac{1}{2}$ and $q_\downarrow = -\frac{1}{2}$. That is, $j_z^\sigma = n + \frac{1}{2}\sigma$, and this also leads to the result that the wave function is single valuedness $\psi_\sigma(\phi + 2\pi) = \psi_\sigma(\phi)$.

An improper result in determining the eigenenergy is due to replacing $j_z^\sigma = n + (1/2)\sigma$ by $j_z = n + (1/2)$ for both spin-up state and spin-down state, then the energy eigenvalue becomes $E_\sigma = \epsilon[\gamma_0 + n + \frac{1}{2} - \sigma\sqrt{|Z|^2 + (b + 1/2)^2}]^2$, which is incorrect. This is because in the absence of spin-orbit interaction, this result will lead to $E_\uparrow = \epsilon(\gamma_0 + n)^2$ and $E_\downarrow = \epsilon(\gamma_0 + n + 1)^2$. That is, $E_\uparrow \neq E_\downarrow$, the energy of the spin-up state will be different from that of the spin-down state even in the absence of the Zeeman interaction, and this is unphysical [38].

In short, we stress that the energy eigenvectors and eigenvalues used in this paper are different from the previous literatures. The discrepancy is due to the total angular momentum $\hat{j}_z = \hat{\ell}_z + (\hbar/2)\sigma_z$, in which the eigenvalue depends on the spin state. For those systems without conservation of angular momentum, the eigenstates should be expanded by the orbital angular momentum states with different quantum number n .

III. INTERNAL ZEEMAN FIELD

In the local Frenet-Serret reference frame [28], the spin orientation is expressed as $\langle \sigma \rangle = \langle \sigma_r \rangle \hat{e}_r + \langle \sigma_\phi \rangle \hat{e}_\phi + \langle \sigma_z \rangle \hat{e}_z$, where the expectation value $\langle \dots \rangle$ is obtained by using the eigenstates of the operator \hat{D}_0 [Eq. (9)], $\hat{D}_0 |\psi_\sigma\rangle = \Lambda_\sigma |\psi_\sigma\rangle$, which can be written as

$$-i \frac{\partial}{\partial s} |\psi_\sigma\rangle = \hat{G}(s) |\psi_\sigma\rangle, \quad (29)$$

where $s = R\phi$ is the arclength of the ring and

$$\hat{G}(s) = \frac{1}{R}(\Lambda_\sigma - \gamma_0) + \frac{1}{R}(-Z_\alpha \sigma_r - Z_\eta \sigma_\phi + b \sigma_z). \quad (30)$$

Therefore the spatial derivation of $\langle \sigma \rangle$ can be written as

$$\frac{\partial}{\partial s} \langle \sigma \rangle = i \langle [\sigma, \hat{G}(\phi)] \rangle + \left\langle \frac{\partial \sigma}{\partial s} \right\rangle. \quad (31)$$

We also note that in the local frame of spin, we have $\partial \sigma_r / \partial \phi = \sigma_\phi$ and $\partial \sigma_\phi = -\sigma_r$. Hence, we obtain

$$\left\langle \frac{\partial \sigma}{\partial s} \right\rangle = \frac{\langle \sigma_\phi \rangle}{R} \hat{e}_r - \frac{\langle \sigma_r \rangle}{R} \hat{e}_z. \quad (32)$$

Equation (32) is independent of spin-orbit interaction. By substitution of Eqs. (30), (7), and (32) into Eq. (31), after a straightforward calculation, we have the following spin-torque equation:

$$\frac{\partial}{\partial s} \langle \sigma \rangle = \mathbf{B}_L \times \langle \sigma \rangle, \quad (33)$$

where \mathbf{B}_L -field is called the effective local field,

$$\mathbf{B}_L = \frac{2Z_\alpha}{R} \hat{e}_r + \frac{2Z_\eta}{R} \hat{e}_\phi + \frac{-2b-1}{R} \hat{e}_z. \quad (34)$$

We note that the external magnetic field \mathbf{B} does not alter the spin orientation because the Zeeman interaction is neglected in the present case. The Rashba-Dirac spin-orbit interaction control an in-plane effective local field. For the energy eigenvectors [Eqs. (21) and (22)], the local spin (σ) can be written as

$$\begin{aligned} \langle \sigma \rangle_\uparrow &\equiv \langle \psi_\uparrow | \sigma | \psi_\uparrow \rangle \\ &= \langle \sigma_r \rangle \hat{e}_r + \langle \sigma_\phi \rangle \hat{e}_\phi + \langle \sigma_z \rangle \hat{e}_z \\ &= (\sin \xi \cos \theta) \hat{e}_r + (\sin \xi \sin \theta) \hat{e}_\phi + (\cos \xi) \hat{e}_z \end{aligned} \quad (35)$$

and $\langle \sigma \rangle_\downarrow = -\langle \sigma \rangle_\uparrow$. We find that

$$\frac{\langle \sigma_\phi \rangle}{\langle \sigma_r \rangle} = \tan \theta. \quad (36)$$

Namely, the in-plane component of spin can be generated by the Dirac type spin-orbit coupling η , which is also similar to the nonconstant curvature of the ring [28]. Importantly, in the absence of spin-orbit interaction, the local field is still nonzero,

$$\mathbf{B}_L = -\frac{1}{R} \hat{e}_z; \quad Z_\alpha = Z_\eta = 0, \quad b = 0, \quad (37)$$

which reveals the presence of an nonvanishing \mathbf{B}_L field in the z direction, and is here-and-after called the internal Zeeman field. When the spin state is taken into account, this internal Zeeman field would change the electronic energy even in the absence of spin-orbit interaction. Interestingly, we find that the internal Zeeman field can be tuned by changing BZ coupling. This enable us to detect the effect of the internal Zeeman field in the ring. When the BZ coupling has a specific value $b = -1/2$, we have

$$\mathbf{B}_L = 0, \quad Z_\alpha = Z_\eta = 0, \quad b = -1/2. \quad (38)$$

By using the form of \mathbf{B}_L field, the energy eigenvalue (27) then can be simplified as $E_\uparrow = \epsilon(\gamma_0 + j_z^\uparrow - |\mathbf{h}|)^2$ and $E_\downarrow = \epsilon(\gamma_0 + j_z^\downarrow + |\mathbf{h}|)^2$, where the \mathbf{h} field is defined as

$$\begin{aligned} \mathbf{h} &= \frac{R}{2} \mathbf{B}_L \\ &= Z_\alpha \hat{e}_r + Z_\eta \hat{e}_\phi - \left(b + \frac{1}{2} \right) \hat{e}_z. \end{aligned} \quad (39)$$

Furthermore, the eigenvalues (27) can be expressed as

$$\begin{aligned} E_{n\sigma} &= \epsilon \left(\gamma_0 + n + \frac{1}{2} \sigma - \sigma |\mathbf{h}| \right)^2 \\ &= \epsilon \left(\gamma_0 + n - \frac{\Phi_\sigma}{2\pi} \right)^2, \end{aligned} \quad (40)$$

where Φ_σ is written as

$$\Phi_\sigma = \sigma \Phi_{AC} \quad (41)$$

and

$$\Phi_{AC} = 2\pi |\mathbf{h}| - \pi \quad (42)$$

is the so-called the AC phase in the ring. It is interesting to note that in the absence of spin-orbit interaction, $|Z| = b = 0$ and we have $|\mathbf{h}| = 1/2$ and the AC phase vanishes $\Phi_{AC} = 0$. However, if the RD coupling vanishes $|Z| = 0$, but the BZ coupling is $b = -1/2$, then $|\mathbf{h}| = 0$ and AC phase is $\Phi_{AC} = -\pi$. In the following section, we will discuss the effect of BZ coupling by calculating the conductance without leads. We close this section by addressing the issues about the modification of energy spectrum. It is easy to show that the symmetry of Eq. (40) is given by

$$\begin{aligned} \gamma_0 &= 0, \quad E_{-n\downarrow} = E_{n\uparrow} \\ \gamma_* &= 0, \quad E_{n\uparrow} = E_{n\downarrow}, \end{aligned} \quad (43)$$

where $\gamma_* = \Phi_{AB}/2\pi$.

In the previous literature, the term Φ_σ in Eq. (40) is expressed as $\Phi_\sigma^o = -\pi(1 - 2\sigma|\mathbf{h}|)$. However, by considering the conserved angular momentum in the present system, the term Φ_σ is written as $\Phi_\sigma = \sigma(-\pi)(1 - 2|\mathbf{h}|)$. In the absence of spin-orbit interaction ($|\mathbf{h}| = 1/2$), we have $\Phi_\sigma = 0$, and energy spectrum goes back to Eq. (14). For the old version, in the absence of spin-orbit interaction ($|\mathbf{h}| = 1/2$), we have $\Phi_\uparrow^o = 0$, but $\Phi_\downarrow^o = -2\pi$. Furthermore, for nonzero spin-orbit interaction ($|Z| \neq 0$ and $b \neq 0$), we have $\Phi_\uparrow^o = \Phi_{AC}$ and $\Phi_\downarrow^o = -\Phi_{AC} - 2\pi$. The additional 2π phase in Φ_\downarrow^o will not have a detectable result in the interference pattern. Although the old energy spectrum is improper, it is still safe to discuss the vanishing spin-orbit interaction in the conductance, which stems from the effect of interference.

IV. CONDUCTANCE

A. Classification of eigenstates

We return to the eigenstates of \hat{J}_z . By observing the total angular momentum quantum number j_z^σ , we found that the energy eigenvectors can be classified by two angular momentum states: parallel and antiparallel orientation of \hat{e}_z and σ_z . For the convenience of description, we write n as $\lambda \bar{n}$, with $\lambda = \pm$ and $\bar{n} = 0, 1, 2, 3, \dots$. The term $\lambda = +$ represents the counterclockwise rotation of an electron and $\lambda = -$ represents the clockwise rotation of an electron. The parallel state is marked by \uparrow , which has two eigenvalues for \hat{J}_z ,

$$\bar{n} + \frac{1}{2}, \quad -\bar{n} - \frac{1}{2}. \quad (44)$$

On the other hand, the antiparallel state is marked by \downarrow , which also has two eigenvalues for \hat{J}_z ,

$$\bar{n} - \frac{1}{2}, \quad -\bar{n} + \frac{1}{2}. \quad (45)$$

Therefore we conclude that the eigenvectors of total angular momentum $|n, \sigma\rangle$ can be classified to $|J, \lambda\rangle$. Namely, we

have¹

$$\begin{aligned} |\bar{n}, \uparrow\rangle &= |\uparrow, +\rangle, & J_z |\uparrow, +\rangle &= (\bar{n} + \frac{1}{2})\hbar |\uparrow, +\rangle, \\ |-\bar{n}, \uparrow\rangle &= |\downarrow, -\rangle, & J_z |\downarrow, -\rangle &= (-\bar{n} + \frac{1}{2})\hbar |\downarrow, -\rangle, \\ |\bar{n}, \downarrow\rangle &= |\downarrow, +\rangle, & J_z |\downarrow, +\rangle &= (\bar{n} - \frac{1}{2})\hbar |\downarrow, +\rangle, \\ |-\bar{n}, \downarrow\rangle &= |\uparrow, -\rangle, & J_z |\uparrow, -\rangle &= (-\bar{n} - \frac{1}{2})\hbar |\uparrow, -\rangle, \end{aligned} \quad (46)$$

where $\bar{n} \geq 0$. The term \uparrow means the orbital angular momentum is parallel to the spin, and \downarrow means the orbital angular momentum is antiparallel to the spin.

We now turn to the energy eigenvectors. Consider parallel states [Eq. (44)], the first state corresponds to $n = +\bar{n}$ and $\sigma = \uparrow$ in Eq. (21), and the second state corresponds to $n = -\bar{n}$ and $\sigma = \downarrow$ in (22). Therefore we have

$$\begin{aligned} |\psi_{\uparrow}^+(\phi)\rangle &= \frac{\exp(i\bar{n}\phi)}{\sqrt{2\pi}} \begin{pmatrix} \cos(\xi/2) \\ \sin(\xi/2)e^{i(\phi+\theta)} \end{pmatrix}, \\ |\psi_{\uparrow}^-(\phi)\rangle &= \frac{\exp(-i\bar{n}\phi)}{\sqrt{2\pi}} \begin{pmatrix} -\sin(\xi/2)e^{-i\phi} \\ \cos(\xi/2)e^{i\theta} \end{pmatrix}. \end{aligned} \quad (47)$$

It can be shown that $|\psi_{\uparrow}^+(\phi)\rangle$ is the eigenvector of the total angular momentum $\hat{J}_z = \hat{L}_z + (\hbar/2)\sigma_z$, i.e., $\hat{J}_z |\psi_{\uparrow}^+(\phi)\rangle = (\bar{n} + 1/2)\hbar |\psi_{\uparrow}^+(\phi)\rangle$. We also have $\hat{J}_z |\psi_{\uparrow}^-(\phi)\rangle = (-\bar{n} - 1/2)\hbar |\psi_{\uparrow}^-(\phi)\rangle$. Because $|\psi_{\uparrow}^+(\phi)\rangle$ and $|\psi_{\uparrow}^-(\phi)\rangle$ correspond to different eigenvalues, they are orthogonal, i.e., it can be shown that $\langle \psi_{\uparrow}^+(\phi) | \psi_{\uparrow}^-(\phi) \rangle = 0$.

Consider antiparallel states [Eq. (44)], the first state corresponds to $n = +\bar{n}$ and $\sigma = \downarrow$ in Eq. (22), and the second state corresponds to $n = -\bar{n}$ and $\sigma = \uparrow$ in (21). Therefore we have

$$\begin{aligned} |\psi_{\downarrow}^+(\phi)\rangle &= \frac{\exp(i\bar{n}\phi)}{\sqrt{2\pi}} \begin{pmatrix} -\sin(\xi/2)e^{-i\phi} \\ \cos(\xi/2)e^{i\theta} \end{pmatrix}, \\ |\psi_{\downarrow}^-(\phi)\rangle &= \frac{\exp(-i\bar{n}\phi)}{\sqrt{2\pi}} \begin{pmatrix} \cos(\xi/2) \\ \sin(\xi/2)e^{i(\phi+\theta)} \end{pmatrix}. \end{aligned} \quad (48)$$

It can be shown that $\hat{J}_z |\psi_{\downarrow}^+(\phi)\rangle = (\bar{n} - 1/2)\hbar |\psi_{\downarrow}^+(\phi)\rangle$ and $\hat{J}_z |\psi_{\downarrow}^-(\phi)\rangle = (-\bar{n} + 1/2)\hbar |\psi_{\downarrow}^-(\phi)\rangle$. Furthermore, we have $\langle \psi_{\downarrow}^+(\phi) | \psi_{\downarrow}^-(\phi) \rangle = 0$. The eigenstate can be written as

$$|\psi_J^\lambda(\phi)\rangle = \frac{\exp(i\lambda\bar{n}'_J\phi)}{\sqrt{2\pi}} |\chi_J^\lambda\rangle, \quad (49)$$

where $J = \uparrow, \downarrow$. In the following section, we calculate the conductance by using the projection operator exhibited by Eqs. (47) and (48).

B. Calculation of conductance

Without leads, the conductance due to the interference of the four total angular momentum states is obtained by

$$G = \frac{e^2}{4h} \sum_{\sigma, \sigma'} |\langle \sigma' | \sigma_{\text{out}} \rangle|^2, \quad (50)$$

¹The completeness of $|J, \lambda\rangle$ is given by $\sum_{J=\uparrow, \downarrow} |J, \lambda\rangle \langle J, \lambda| = 1$ and $\sum_{\lambda=+, -} |J, \lambda\rangle \langle J, \lambda| = 1$.

where $\sigma = \uparrow, \downarrow$ and the factor 4 means that there are four available channels of the quantum ring. The mixed total angular momentum state leave the ring at $\phi = \pi$, and we have

$$|\sigma_{\text{out}}\rangle = \sum_{J, \lambda} e^{i\bar{n}'_J\pi} |\chi_J^\lambda(\pi)\rangle \langle \chi_J^\lambda(0) | \sigma \rangle, \quad (51)$$

where $J = \uparrow, \downarrow$ and the sign $\lambda = \pm$ represents the direction of the channels. We note that because the injection of spin in the ring should obey the conservation of total angular momentum, the projection operator should be constructed by the parallel and antiparallel states. This is because, for example, an up spin in the ring will transport only through upper channel (parallel state) or lower channel (antiparallel state). By using the completeness $\sum_{\sigma} |\sigma\rangle \langle \sigma| = 1$, Eq. (50) can be written as

$$G = \frac{e^2}{4h} \sum_{\lambda, J} \sum_{\lambda', J'} \langle \chi_J^\lambda(0) | \chi_{J'}^{\lambda'}(0) \rangle \langle \chi_{J'}^{\lambda'}(\pi) | \chi_J^\lambda(\pi) \rangle e^{i(n'_J - n'_{J'})\pi}. \quad (52)$$

By using Eqs. (47) and (48) into Eq. (52), and after straightforward calculations, we obtain

$$G = \frac{e^2}{h} \left\{ 1 + \frac{1}{2} [\cos(\bar{n}_+^{\uparrow}\pi - \bar{n}_-^{\downarrow}\pi) + \cos(\bar{n}_+^{\downarrow}\pi - \bar{n}_-^{\uparrow}\pi)] \right\}. \quad (53)$$

The first term in the bracket $[\dots]$ of Eq. (53) corresponds to the interference of only spin-up wave function, and the second term corresponds to the interference of only the spin-down wave function as shown in Fig. 2(b).

Importantly, we note that Eq. (53) was discussed in the previous papers [25,39]. However, we note that the orbital quantum number is related to the parallel and antiparallel states, but not the spin angular momentum. The orbital quantum number n'_λ are

$$\begin{aligned} \bar{n}_+^{\uparrow} &: \bar{n} + \frac{1}{2}, & \bar{n}_-^{\uparrow} &: -\bar{n} - \frac{1}{2}, \\ \bar{n}_+^{\downarrow} &: \bar{n} - \frac{1}{2}, & \bar{n}_-^{\downarrow} &: -\bar{n} + \frac{1}{2}. \end{aligned} \quad (54)$$

We stress that the state \uparrow does not mean the spin is in the up state, and vice versa. We note that, \bar{n}_+^{\uparrow} represents $n = +\bar{n}$ and $\sigma = \uparrow$, and the corresponding energy is $\epsilon(\gamma_0 + \bar{n}_+^{\uparrow} + 1/2 - |\mathbf{h}|)^2$. On the other hand, \bar{n}_-^{\downarrow} represents $n = -\bar{n}$ and $\sigma = \uparrow$, and the corresponding energy is $\epsilon(\gamma_0 - \bar{n}_-^{\downarrow} + 1/2 - |\mathbf{h}|)^2$, and so on. The corresponding eigenvalues are

$$\begin{aligned} \bar{n}_+^{\uparrow} &: E_{\uparrow}^+ = \epsilon(\gamma_0 + \bar{n}_+^{\uparrow} + \frac{1}{2} - |\mathbf{h}|)^2, \\ \bar{n}_-^{\uparrow} &: E_{\uparrow}^- = \epsilon(\gamma_0 - \bar{n}_-^{\uparrow} - \frac{1}{2} + |\mathbf{h}|)^2, \\ \bar{n}_+^{\downarrow} &: E_{\downarrow}^+ = \epsilon(\gamma_0 + \bar{n}_+^{\downarrow} - \frac{1}{2} + |\mathbf{h}|)^2, \\ \bar{n}_-^{\downarrow} &: E_{\downarrow}^- = \epsilon(\gamma_0 - \bar{n}_-^{\downarrow} + \frac{1}{2} - |\mathbf{h}|)^2. \end{aligned} \quad (55)$$

By imposing the Fermi energy to the energy eigenvalue, $E_s^\lambda = E_F$, we have $E_F/\epsilon = (\gamma_0 + \bar{n}_+^{\uparrow} + 1/2 - |\mathbf{h}|)^2 = (\gamma_0 - \bar{n}_-^{\downarrow} + 1/2 - |\mathbf{h}|)^2$. Simple algebraic calculations, we have

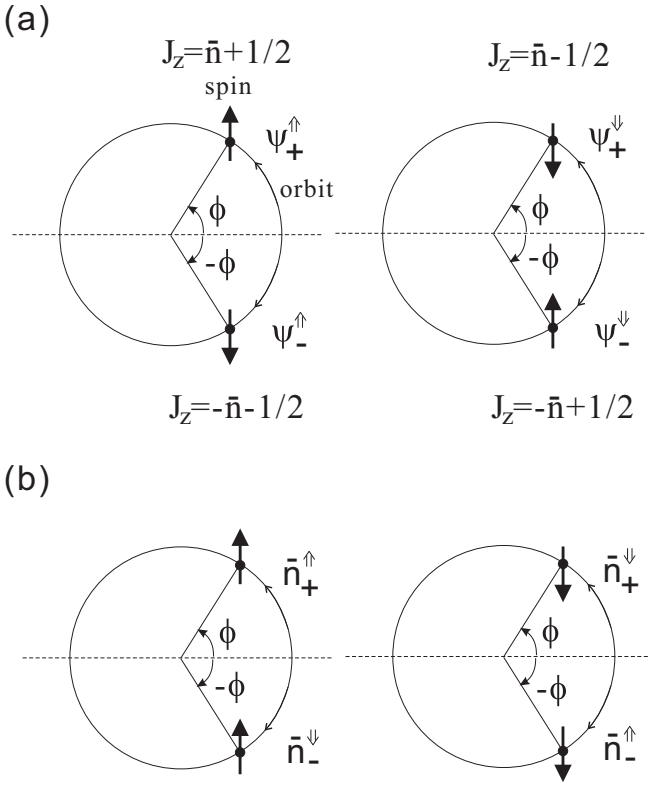


FIG. 2. (a) Schematic diagram showing the parallel (left) and antiparallel (right) states defined in Eq. (46). (b) Schematic diagram showing the spin up (left) and spin down (right) states. The interference is within each spin state, as given by Eq. (53).

$(\bar{n}_+^\uparrow + \bar{n}_-^\downarrow)(\bar{n}_+^\uparrow - \bar{n}_-^\downarrow + 1 - 2|\mathbf{h}| + 2\gamma_0) = 0$. This implies

$$\begin{aligned} \bar{n}_+^\uparrow - \bar{n}_-^\downarrow &= 2|\mathbf{h}| - 1 - 2\gamma_0 \\ &= \frac{\Phi_{AC}}{\pi} - 2\gamma_0. \end{aligned} \quad (56)$$

Furthermore, we also have

$$\begin{aligned} \bar{n}_+^\downarrow - \bar{n}_-^\uparrow &= 1 - 2|\mathbf{h}| - 2\gamma_0 \\ &= -\frac{\Phi_{AC}}{\pi} - 2\gamma_0. \end{aligned} \quad (57)$$

Because we neglect the Zeeman term that couples the spin and external magnetic field, the phase change is attributed to pure spin part (AC phase Φ_{AC}) and pure electronic part (magnetic flux $2\pi\gamma_0$). For the external magnetic flux, the phase $2\pi\gamma_0$ due to the pure electronic properties is the same for spin up and spin down states. The difference is the phase caused by the spin-orbit interaction, the AC phase acquired by spin up state is opposite to that by spin-down state. Equation (53) becomes

$$\begin{aligned} G &= \frac{e^2}{h} \left\{ 1 + \frac{1}{2} [\cos(\Phi_{AC} - 2\pi\gamma_0) + \cos(\Phi_{AC} + 2\pi\gamma_0)] \right\} \\ &= \frac{e^2}{h} \{ 1 + \cos(2\pi\gamma_0) \cos \Phi_{AC} \}. \end{aligned} \quad (58)$$

Equation (58) is one of the main results in this paper, which is a periodic oscillation exhibited by γ_0 and Φ_{AC} . We also note

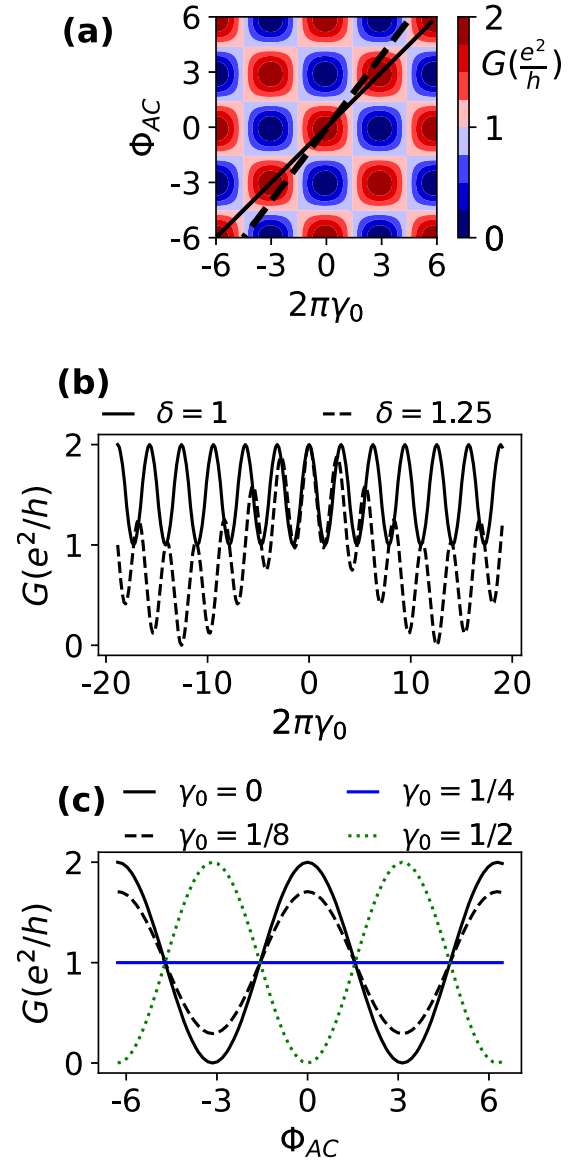


FIG. 3. (a) the conductance Eq. (58) as a function of the magnetic flux $2\pi\gamma_0$ and the AC phase Φ_{AC} ; (b) the conductance with $\Phi_{AC} = \delta Q_0$ and $Q_0 = 2\pi\gamma_0$, where $\delta = 1$ and $\delta = 1.25$ correspond to the solid line and dashed line in (a), respectively; (c) the conductance v.s. the AC phase for different values of magnetic flux γ_0 . For the one-quarter quantum flux, $\gamma_0 = 1/4$, the conductance is a constant regardless of the strength of spin-orbit interaction.

that the conductance (58) is similar to the result in the hole ring [31]. Equation (58) as a function of γ_0 and Φ_{AC} is plotted in Fig. 3(a).

If the phase of magnetic flux is equal to the AC phase (mod 2π), i.e., $Q_0 \equiv 2\pi\gamma_0 = \pm\Phi_{AC}$, then the conductance becomes

$$G = \frac{e^2}{h} \{ 1 + \cos^2 Q_0 \pi \}, \quad Q_0 \pi = 2\pi\gamma_0 = \pm\Phi_{AC}.$$

The Q_0 value corresponds to the off-diagonal line of the Fig. 3(a) with positive slope or negative slope. The minima of G is e^2/h and the maxima is $2e^2/h$. Interestingly, we set

$\Phi_{AC} = \delta Q_0$ and $2\pi\gamma_0 = Q_0$, and the conductance becomes

$$G = \frac{e^2}{h} \left\{ 1 + \frac{1}{2} [\cos((\delta - 1)Q_0) + \cos((\delta + 1)Q_0)] \right\}. \quad (59)$$

The resulting conductance is plotted in Fig. 3(b). We find that when $\delta = 1.25$ [along the dashed line in Fig. 3(a)], the conductance has the beat phenomenon. An important result from the beat phenomena is that the conductance can vary periodically without passing the insulating state.

When γ_0 is an one-quarter quantum flux, $\gamma_0 = \pm 1/4, \pm 3/4, \pm 5/4, \dots$, then the conductance remains constant $G = e^2/h$, regardless of the strength of spin-orbit interaction as shown in Fig. 3(c). This is because the phase accumulated by an electron is $e^{i\gamma_0\phi}$ for a travel through angle ϕ . The accumulated phase of the electronic wave function through the ring is $e^{i2\pi\gamma_0}$ and the resulting interference is $\cos(2\pi\gamma_0)$. The magnetic flux $\gamma_0 = 1/4$ leads to the complete destructive interference for both spin-up and spin-down electrons. Therefore the conductance contains only four channels with pure electronic transport, i.e., $G = (e^2/4h) \times 4 = e^2/h$. Moreover, if Φ_{AC} shows half-integer numbers, $\Phi_{AC} = \pm\pi/2, \pm 3\pi/2, \pm 5\pi/2$, then the conductance also becomes a constant $G = e^2/h$ regardless of the strength of the magnetic flux.

In the absence of magnetic flux, $\gamma_0 = 0$, the conductance Eq. (58) becomes

$$G_0 = \frac{e^2}{h} \{1 + \cos \Phi_{AC}\}. \quad (60)$$

Equation (60) was obtained in the previous works by many authors (Refs. [39,40] and other reference therein). Our result shows that Eq. (58) goes back to Eq. (60) not only when the magnetic flux vanishes but an integer number $\gamma_0 = 0, \pm 1, \pm 2, \dots$. However, unlike the result Eq. (60), for half-integer numbers $\gamma_0 = \pm 1/2, \pm 3/2, \pm 5/2, \dots$, Eq. (58) gives a rather different result,

$$G_{1/2} = \frac{e^2}{h} \{1 - \cos \Phi_{AC}\}. \quad (61)$$

From Eqs. (60) and (61), we can obtain the AC phase by measuring G_0 and $G_{1/2}$,

$$\Phi_{AC} = \cos^{-1} \left(\frac{G_0 - G_{1/2}}{G_0 + G_{1/2}} \right). \quad (62)$$

Equation (62) enables us to detect the existence of the internal Zeeman field in the quantum ring.

C. Effect of only BZ coupling

In this section, we discuss the conductance in the absence of Rashba and Dirac-type coupling, $Z_\alpha = Z_\eta = 0$. The AC phase becomes

$$\Phi_{AC} = 2\pi \left| b + \frac{1}{2} \right| - \pi. \quad (63)$$

If we further turn off the BZ coupling ($b = 0$), this leads to $\Phi_{AC} = 0$, and the conductance [Eq. (58)] is given by

$$G = \frac{e^2}{h} [1 + \cos(2\pi\gamma_0)]. \quad (64)$$

In this case, in the absence of external magnetic field ($\gamma_0 = 0$), the conductance is the maximum value $G = 2e^2/h$. Nevertheless, if the BZ coupling exactly cancels the internal Zeeman field, $(b + 1/2) = 0$, then $\Phi_{AC} = -\pi$ and the conductance [Eq. (58)] becomes

$$G = \frac{e^2}{h} [1 - \cos(2\pi\gamma_0)]. \quad (65)$$

We find that in this case, the conductance vanishes even in the absence of an external magnetic field (and integer flux quantum, $\gamma_0 = \pm 1, \pm 2, \pm 3, \dots$). The conductance goes back to $2e^2/h$ when γ_0 is an half-integer number $\gamma_0 = \pm 1/2, \pm 3/2, \pm 5/2, \dots$

If the BZ coupling is zero, Eq. (60) leads to $G_0 = 2e^2/h$, however, Eq. (61) leads to vanishing conductance $G_{1/2} = 0$. Inversely, the cancellation of internal Zeeman field ($\Phi_{AC} = -\pi$) implies that $G_0 = 0$ and $G_{1/2} = 2e^2/h$. Therefore we conclude that

$$b = 0 \begin{cases} G = 0, & \gamma_0 = \pm 1/2, \pm 3/2, \dots \\ G = 2e^2/h, & \gamma_0 = 0, \pm 1, \pm 2, \dots \end{cases} \quad (66)$$

and

$$(b + 1/2) = 0 \begin{cases} G = 0, & \gamma_0 = 0, \pm 1, \pm 2, \dots \\ G = 2e^2/h, & \gamma_0 = \pm 1/2, \pm 3/2, \dots \end{cases} \quad (67)$$

The difference between the vanishing spin-orbit interaction and the cancellation of internal Zeeman field can be observed by using integer magnetic flux and half-integer magnetic flux.

D. Effect of RD coupling

In the presence of both Rashba-Dirac and BZ coupling, the \mathbf{h} -field $|\mathbf{h}| = \sqrt{|Z|^2 + (b + 1/2)^2}$ indicates that $|Z|^2$ and $(b + 1/2)^2$ plays the same role in Φ_{AC} . For a fixed γ_0 , the conductance behaves like a spherical wave due to the point source, where the location of the source point is at $b = -1/2$ and $|Z| = 0$, as shown in Fig. 4. The change of magnetic flux from integer to half-integer can alter the maximum and minimum positions. Because of the width between maximum values in the pattern of conductance, when $b + 1/2 \neq 0$ the conductance can have a quasiplateau in $|Z|$. In Fig. 4, we find that the BZ interaction b can change the width of the quasiplateau of the conductance. For larger values of BZ coupling, we could have a wider plateau in conductance.

On the other hand, as shown in Fig. 5, if the BZ coupling cancels the internal Zeeman field ($b + 1/2 = 0$), then the conductance is still a periodic function of $|Z|$ as well as γ_0 . The plateau appears when $b = 0$, i.e., the internal Zeeman field is non zero. When we increase the value of the BZ coupling, which is equivalent to enhance the internal Zeeman field, and the plateau becomes larger. Because of the periodicity of the conductance, the quasiplateau could be a conducting state or an insulating state regardless of the small change in the RD coupling $|Z|$.

V. PERSISTENT SPIN CURRENT AT LOW TEMPERATURE

It is known that the AC effect manifests the persistent spin current in the ring with spin-orbit coupling [41,42]. In this section, we calculate the spin current by using canonical partition function [42]. The orbital angular momentum $\hat{\ell}_z$ is

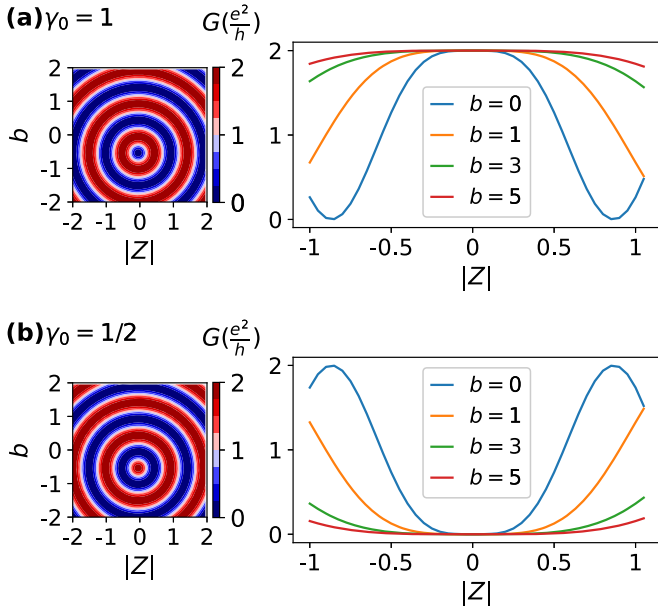


FIG. 4. Figures showing the influence of the spin-orbit interaction to the conductance, we use (a) $\gamma_0 = 1$ and (b) $1/2$. The location of conductance maximum and minimum interchanged in (a) and (b) as a result of the phase difference π .

the generalized momentum in Hamiltonian \hat{H}_0 , which is denoted as $p_\phi = \hat{\ell}_z = -i\hbar\partial/\partial\phi$. The velocity operator is given by

$$\begin{aligned} \hat{v} &= \frac{\partial \hat{H}_0}{\partial p_\phi} \\ &= \epsilon \left\{ \frac{\partial \hat{D}_0}{\partial p_\phi}, \hat{D}_0 \right\} = \frac{2\epsilon}{\hbar} \hat{D}_0, \end{aligned} \quad (68)$$

where the notation $\{A, B\} = AB + BA$ was used. The conventional definition of spin current is $\mathcal{J}_s^z = \frac{1}{2}\{\hat{v}, \frac{\hbar}{2}\sigma_z\}$, and we have

$$\begin{aligned} \mathcal{J}_s^z &= \frac{1}{2} \left\{ \hat{v}, \frac{\hbar}{2} \sigma_z \right\} \\ &= \epsilon \left[\left(\frac{\hat{\ell}_z}{\hbar} + \gamma_0 \right) \sigma_z - b \right], \end{aligned} \quad (69)$$

where $\{\sigma_r, \sigma_z\} = 0$ and $\{\sigma_\phi, \sigma_z\} = 0$ were used. The thermal equilibrium expectation value (thermal average) $\langle \mathcal{O} \rangle_\beta$ of the

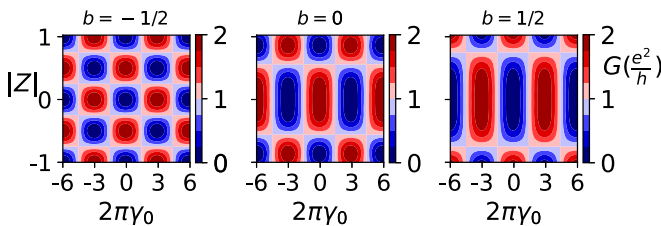


FIG. 5. Figures showing the influence of the BZ coupling to the conductance in the presence of Rashba-Dirac coupling. From left to right, the value of the BZ interaction is $-1/2$, 0 , $1/2$, respectively.

observable \mathcal{O} is given by the canonical ensemble,

$$\begin{aligned} \langle \mathcal{O} \rangle_\beta &= \frac{1}{\mathcal{Z}} \text{Tr}[e^{-\beta \hat{H}_0} \mathcal{O}] \\ &= \frac{1}{\mathcal{Z}} \sum_{n=-\infty}^{\infty} \sum_{\sigma} e^{-\beta E_{n\sigma}} \langle \psi_{n\sigma} | \mathcal{O} | \psi_{n\sigma} \rangle, \end{aligned} \quad (70)$$

where $\langle \psi_{n\sigma} | \mathcal{O} | \psi_{n\sigma} \rangle$ is the quantum mechanical average

$$\langle \psi_{n\sigma} | \mathcal{O} | \psi_{n\sigma} \rangle = \int_0^{2\pi} d\phi \psi_{n\sigma}^\dagger(\phi) \mathcal{O} \psi_{n\sigma}(\phi) \quad (71)$$

and the partition function \mathcal{Z} reads

$$\mathcal{Z} = \text{Tr}[e^{-\beta \hat{H}_0}] = \sum_{n=-\infty}^{\infty} \sum_{\sigma} e^{-\beta E_{n\sigma}}. \quad (72)$$

We find that the quantum mechanical average of spin components satisfy² $\langle \psi_{n\sigma} | \sigma_x | \psi_{n\sigma} \rangle = \langle \psi_{n\sigma} | \sigma_y | \psi_{n\sigma} \rangle = 0$ and $\langle \psi_{n\sigma} | \sigma_z | \psi_{n\sigma} \rangle = \sigma \cos \xi$. In the presence of external magnetic flux ($\gamma_0 \neq 0$), the thermal average of spin current is given by (after some straightforward calculations)

$$\langle \mathcal{J}_s^z \rangle_\beta = \epsilon \bar{J}_s, \quad \bar{J}_s = \frac{\mathcal{P}_\uparrow - \mathcal{P}_\downarrow}{\mathcal{Z}_\uparrow + \mathcal{Z}_\downarrow} \cos \xi, \quad (73)$$

where $\gamma_* = \Phi_{AC}/2\pi$, ϵ is defined in Eq. (8),

$$\cos \xi = \frac{b + 1/2}{\sqrt{|Z|^2 + (b + 1/2)^2}}, \quad (74)$$

and

$$\begin{aligned} \mathcal{P}_\uparrow &= \sum_{n=-\infty}^{\infty} (n + \gamma_0 - \gamma_*) e^{-\beta E_{n\uparrow}}, \\ \mathcal{P}_\downarrow &= \sum_{n=-\infty}^{\infty} (n + \gamma_0 + \gamma_*) e^{-\beta E_{n\downarrow}}, \\ \mathcal{Z}_\uparrow &= \sum_{n=-\infty}^{\infty} e^{-\beta E_{n\uparrow}}, \quad \mathcal{Z}_\downarrow = \sum_{n=-\infty}^{\infty} e^{-\beta E_{n\downarrow}}, \end{aligned} \quad (75)$$

where $E_{n\uparrow(\downarrow)}$ are defined in Eq. (40). Until now no approximations have been done in deriving Eq. (73). The nonzero value of Eq. (73) is the so-called persistent spin current. Here-and-after we simply call $\langle \mathcal{J}_s^z \rangle_\beta$ the spin current and \bar{J}_s is called the scaled spin current.

In the absence of magnetic flux $\gamma_0 = 0$, it can be shown that Eq. (73) reproduces the result shown in Ref. [42], but the energy spectrum is different. Furthermore, in this case, we have $E_{-n\downarrow} = E_{n\uparrow}$ [see also Eq. (43)], and thus, the thermal average of spin vanishes $\langle \sigma \rangle_\beta = 0$. However, the thermal average of the spin current $\langle \mathcal{J}_s^z \rangle_\beta$ would be nonzero as has been shown in Ref. [42].

²The expectation value of spin x component by using a spinor is given by $\psi_{n\sigma}^\dagger(\phi) \sigma_x \psi_{n\sigma}(\phi) = (\sigma/2\pi) \sin \xi \cos(\theta + \phi)$, and thus, it vanishes because of the cylindrical symmetry $\int_0^{2\pi} d\phi \psi_{n\sigma}^\dagger \sigma_x \psi_{n\sigma} = 0$. For y component, we have $\psi_{n\sigma}^\dagger \sigma_y \psi_{n\sigma}(\phi) = (\sigma/2\pi) \sin \xi \sin(\theta + \phi)$, and we also have a vanishing spin y component $\int_0^{2\pi} d\phi \psi_{n\sigma}^\dagger \sigma_y \psi_{n\sigma} = 0$.

TABLE I. The thermal average of spin and charge currents [Eqs. (73) and (78)] for cases of vanishing spin-orbit interaction $\gamma_* = 0$, vanishing magnetic flux $\gamma_0 = 0$, and vanishing internal Zeeman field $b + 1/2 = 0$. The symbol “0” means always zero, and the symbol “ \times ” means nonzero in general except to the nodelike lines.

	$\gamma_* = 0$	$\gamma_0 = 0$	$b + 1/2 = 0$
$\langle \mathcal{J}_s^z \rangle_\beta$	0	\times	0
$\langle \mathcal{J}_e \rangle_\beta$	\times	0	\times

Looking at Eqs. (73) and (74), some simple relations between spin current and γ_0 and γ_* are apparent. In the absence of spin-orbit interaction ($\gamma_* = 0$), the internal Zeeman field still tilt spin with an angle $\xi = 0$. However, in this case we have $E_{n\uparrow} = E_{n\downarrow} = \epsilon(n + \gamma_0)^2$, and the thermal average gives $\mathcal{P}_\uparrow = \mathcal{P}_\downarrow$. Therefore the spin current vanishes even in the presence of magnetic flux ($\gamma_0 \neq 0$). Furthermore, if BZ coupling exactly cancels the internal Zeeman field $b + 1/2 = 0$, we have $\cos \xi = 0$ for $|Z| \neq 0$. That is, the spin current also vanishes regardless of the strength of Rashba-Dirac spin-orbit interaction (see also Table I). Except to the cancellation of internal Zeeman field and vanishing spin-orbit interaction, the spin current would be nonzero. We note that the transmission of spinful electrons in a single ring with metallic-like contact at high temperature was investigated in Ref. [43], which showed that in the Rashba system spin interference effects are not suppressed by the thermal average.

In the present case, we discuss this phenomenon at low temperature in the following subsections. The energy scale of the quantum ring is $\epsilon = \hbar^2/2mR$ which is about 6.5×10^{-5} eV for InAs ring with $R \approx 1 \mu\text{m}$. Therefore, for the low temperature $T \approx 10^{-3}$ K, we have $\beta\epsilon \approx 100$, which will necessitate summing only finite values of n , and make the computation feasible.

A. In the presence of only BZ coupling

This subsection is to numerically calculate Eq. (73) in the presence of only BZ coupling, i.e., $|Z| = 0$. In this case, we have $\gamma_* = |b + 1/2| - 1/2$ and $\cos \xi = (b + 1/2)/|b + 1/2|$. For the convenience of discussion, we focus on the value of $b + 1/2 \geq 0$. The cosine of the tilt angle $\cos \xi$, which is a sign function of $(b + 1/2)$, is always positive in the range of b discussed. We also discuss small changes in BZ coupling near by $b = -1/2$, and the value $\gamma_* = b$ ranges from $-1/2$ to 1 . The scaled spin current [\bar{J}_s in Eq. (73)] becomes

$$\bar{J}_s = \frac{\mathcal{P}_\uparrow - \mathcal{P}_\downarrow}{\mathcal{Z}_\uparrow + \mathcal{Z}_\downarrow}. \quad (76)$$

The numerical results of Eq. (76) at low temperature is shown in Fig. 6(a), which we take the value $\beta\epsilon = 100$ in our calculation. Because the large value of $\beta\epsilon$, the contribution of terms of large n are neglected. In the present calculation, the maximum n is 10. We observe that the spin current is a periodic function of BZ coupling b and magnetic flux γ_0 . At those values of $b = -1/2, 0, 1/2, 1$, the spin currents are vanishingly small regardless of the strength of magnetic flux. For upper subfigure in Fig. 6(a), we find that the spin current has abrupt changes near $b = -1/2$ and $b = 1/2$ when $\gamma_0 = 0$,

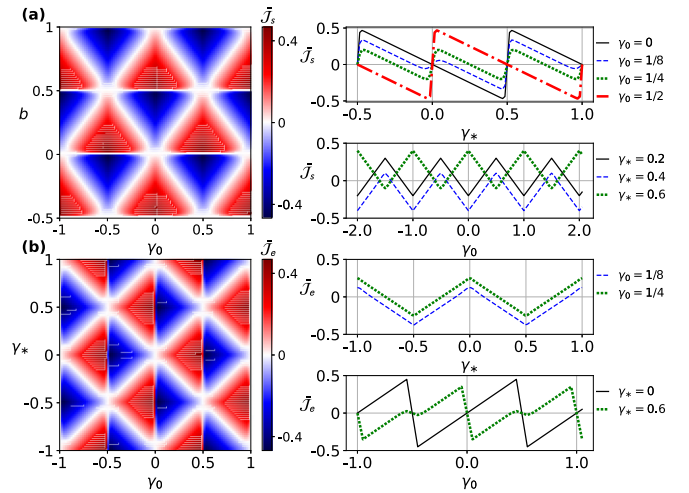


FIG. 6. (a) Numerical results of the persistent spin current [Eq. (76), $\bar{J}_s \equiv \langle \mathcal{J}_s^z \rangle_\beta / \epsilon$] for $Z = 0$ as a function of γ_0 and b . The upper (lower) subfigure showing \bar{J}_s as a function of BZ coupling b (γ_0) with different values of γ_0 (BZ coupling b). The nodelike lines at $b = 1, 0.5, 0, -0.5, -1$ are parallel to the axis of γ_0 . (b) Numerical results of the charge current [Eq. (78), $\bar{J}_e \equiv \langle \mathcal{J}_e \rangle_\beta / (2e\epsilon/\hbar)$] as a function of magnetic flux γ_0 and AC phase γ_* . The upper (lower) subfigure showing \bar{J}_e as a function of γ_* (γ_0) with different values of γ_0 (γ_*). The nodelike lines at $\gamma_0 = -1, -0.5, 0, 0.5, 1$ are perpendicular to the axis γ_0 .

which is similar to the result observed in Ref. [42]. We find that when the magnetic flux increases, the spin current decreases and these abrupt changes shifts to the locations $\gamma_0 = 0$ and $\gamma_0 = 1/2$. For lower subfigure in Fig. 6(a), the persistent spin current has a zigzaglike change with the changing of magnetic flux. The increase of BZ coupling ($b = \gamma_*$) also results in the shift of the magnitude of the spin current, but the tip positions of the zigzaglike shape do not have explicit change.

B. Persistent spin current without charge current

We start from the charge current operator that is given by

$$\mathcal{J}_e = e\hat{v} = \frac{2e\epsilon}{\hbar} \hat{h}_0, \quad (77)$$

where the velocity operator [Eq. (68)] was used. After straightforward calculation, the thermal averaged the charge current (simply called charge current) is

$$\langle \mathcal{J}_e \rangle_\beta = \frac{2e\epsilon}{\hbar} \bar{J}_e, \quad \bar{J}_e = \frac{\mathcal{P}_\uparrow + \mathcal{P}_\downarrow}{\mathcal{Z}_\uparrow + \mathcal{Z}_\downarrow}. \quad (78)$$

In the absence of spin-orbit interaction ($\gamma_* = 0$), we have $\mathcal{P}_\uparrow = \mathcal{P}_\downarrow$, Eq. (78) shows that the charge current is in general nonzero, but the spin current [Eq. (73)] vanishes. On the other hand, \bar{J}_e in Eq. (78) can be written as

$$\begin{aligned} \bar{J}_e &= \gamma_0 + \frac{1}{Z} \sum_{n=-\infty}^{\infty} n (e^{-\beta E_{n\uparrow}} + e^{-\beta E_{n\downarrow}}) \\ &+ \frac{\gamma_*}{Z} \sum_{n=-\infty}^{\infty} (e^{-\beta E_{n\uparrow}} - e^{-\beta E_{n\downarrow}}), \end{aligned} \quad (79)$$

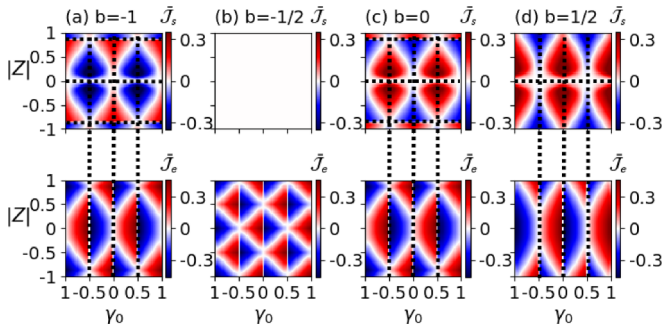


FIG. 7. Numerical results of both charge current \bar{J}_e and spin current \bar{J}_s [Eq. (73), $\cos \xi$ is taken into account] as a function of magnetic flux γ_0 and Rashba-Dirac coupling $|Z|$ for $b = -1, -1/2, 0, 1/2$. We note that the choice of b in the present case leads to an additional nodelike line at $|Z| = 0$ [see Fig. 6(a)]. For other choice of b , there is in general no nodelike line at $|Z| = 0$.

where \bar{J}_e is called the scaled charge current. In the absence of magnetic flux $\gamma_0 = 0$, we have $E_{-n\downarrow} = E_{n\uparrow}$ [see also Eq. (43)], and thus the second line of Eq. (79) vanishes. Moreover, follow the same reason, we have $\sum_{n=-\infty}^{+\infty} ne^{-\beta E_{n\downarrow}} = \sum_{n=-\infty}^{+\infty} (-n)e^{-\beta E_{n\uparrow}}$ by using the change of dummy index $n \rightarrow -n$. The second term of the first line of Eq. (79) also vanishes. As a result, the thermal average of the charge current always vanishes in the absence of the magnetic flux (see also Table I).

Similar to the thermal average of spin current, we find that the interference that stems from γ_0 and γ_* is not suppressed by the thermal average. Interestingly, from Fig. 6(b), we observe that the charge current always vanishes at half-integer magnetic flux ($\gamma_0 = 0, \pm 1/2, \pm 1, \dots$) forming nodelike lines and independent of spin-orbit interaction. This is similar to the spin current, there exists nodelike lines of γ_* that results in vanishing spin current regardless of the magnetic flux. We will go back to this point later. Furthermore, parallel to these nodelike lines, the charge current as a function of γ_* has a zigzag structure [see upper subfigure in Fig. 6(b)]. Perpendicular to the nodelike lines, the charge current has abrupt changes [see lower subfigure in Fig. 6(b)].

Explicitly, compare Fig. 6(a) with Fig. 6(b), we find that the nodelike lines of spin current is perpendicular to that of the charge current. Alternatively, we further plot the charge and spin currents as a function of the magnetic flux γ_0 and Rashba-Dirac coupling $|Z|$ for various BZ couplings at low temperature ($\beta\epsilon = 100$), as shown in Fig. 7. The dashed lines locate the zero charge and spin current.

The nodelike lines of spin current are perpendicular to that of the charge current. The positions of nodelike lines exhibited by the AC phase γ_* changes with the strength of the spin-orbit interaction, but the nodelike lines of the charge current are fixed for γ_0 . Therefore we conclude that when magnetic flux is half-integer numbers ($\gamma_0 = 0, \pm 1/2, \pm 1, \dots$), the charge current vanishes but the spin current does not vanish in general (except to its nodelike lines) and vice versa. Interestingly, because of the perpendicular node phenomenon, there exists some points (nonzero γ_0 and nonzero $|Z|$) that both spin and charge currents vanish.

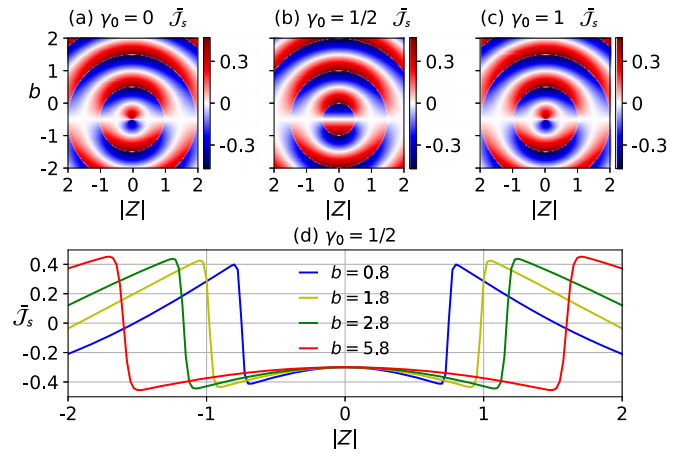


FIG. 8. Spin current \bar{J}_s [Eq. (73), $\cos \xi$ is taken into account] as a function of Rashba-Dirac coupling $|Z|$ and BZ coupling for (a) $\gamma_0 = 0$, (b) $\gamma_0 = 1/2$, (c) $\gamma_0 = 1$, where the charge currents all vanishes. Numerically, we find that (a) is the same as (c), and thus, the spin current has a period $\phi_0/2$. For (d) $\gamma_0 = 1/2$, plateaulike spin current is exhibited by the increase in the BZ coupling.

We emphasize that the BZ coupling is not the key point in generating pure spin current, but the internal Zeeman field. As shown in Figs. 8(a)–8(c) (see also Fig. 7 for $b = 0$), the charge currents are zero and only spin current survives. For $b = 0$, the spin current is still nonzero in general. By inspection of Fig. 8, the spin current has the similar concentric circular structure as the conductance in Fig. 4. It follows that we also have the quasiplateau structure in spin current. For instance, consider Fig. 8(b), we find that the pure spin current regime is broader for large BZ coupling than for the small BZ coupling, as shown in Fig. 8(d).

The charge and spin current have been investigated in previous studies. In Ref. [14], flux dependencies of charge and spin currents were investigated, where the electron number and barrier strength were taken into account. The pure spin current could be generated in a quantum ring. In Ref. [44], the authors showed that the pure spin current can appear within a quantum ring with Rashba spin-orbit interaction under finite bias. In contrast to previous studies, our results point out the effect of internal Zeeman field and show that the interference survives thermal average.

VI. CONCLUSION

In this paper, we investigate Rashba-Dirac (RD) and Bernevig-Zhang (BZ) spin-orbit coupling in the quantum ring. The conservation of total angular momentum was taken into account in obtaining energy eigenvalues and eigenvectors. The wave function is classified to parallel and antiparallel states. We found that the resulting conductance depends on both the external magnetic flux and Aharonov-Casher (AC) phase. The beat behavior of the conductance shows that the conductance can oscillate without passing insulating states. Interestingly, when the magnetic flux is one-quarter flux quantum, the conductance is a constant regardless of the strength of RD-BZ spin-orbit interaction. We also found that the internal Zeeman field can be changed by tuning the BZ coupling. By

using the fractional magnetic flux (integer and half-integer), we can distinguish the difference between vanishing BZ coupling and the cancellation of the internal Zeeman field. We also showed that the existence of internal Zeeman field and BZ coupling can result in the quasiplateau in conductance near the weak Rashba-Dirac coupling regime. Furthermore, the increase in BZ coupling leads to the wider quasiplateau. The quasiplateau of the ring in the large BZ coupling could be at conducting state or insulating state, which triggered by the integer and half-integer magnetic flux. Moreover, the persistent spin and charge currents are nonzero even after thermal average. By tuning the magnetic flux and the spin-orbit interaction, the pure spin current with vanishing charge current can be achieved. Similar to the quasiplateau in conductance, the persistent and pure spin current regime (as a function of RD coupling) is broader in strong BZ coupling than in the weak BZ coupling.

ACKNOWLEDGMENTS

T.-W.C. particularly would like to thank Tsu-Hui Meng for helpful discussions on the dynamics of spin on the ring. H.-C.H. acknowledges the support from the National Science and Technology Council (NSTC) of Taiwan under Grant No. 111-2112-M-004-008.

APPENDIX A: DERIVATIONS OF EQ. (8) AND (9)

In this Appendix, we will derive Eqs. (8) and (9) from Eq. (5) by using the method shown in Ref. [26]. For the convenience of reading, we repeat the two equations (8) and (9) here,

$$\hat{H}_0 = \epsilon \hat{D}_0^2, \quad \epsilon = \frac{\hbar^2}{2mR^2}, \quad (\text{A1})$$

where the operator \hat{D}_0 is given by

$$\hat{D}_0 = \frac{\hat{\ell}_z}{\hbar} + \gamma_0 + Z_\alpha \sigma_r + Z_\eta \sigma_\phi - b\sigma_z. \quad (\text{A2})$$

We define a new operator $\hat{L}_z = \frac{\hat{\ell}_z}{\hbar} + \gamma_0$, and \hat{D}_0^2 can be written as

$$\begin{aligned} \hat{D}_0^2 &= (\hat{L}_z + Z_\alpha \sigma_r + Z_\eta \sigma_\phi - b\sigma_z)^2 \\ &= (\hat{L}_z + Z_\alpha \sigma_r + Z_\eta \sigma_\phi)^2 - b\{\sigma_z, Z_\alpha \sigma_r + Z_\eta \sigma_\phi\} \\ &\quad - 2b\sigma_z \hat{L}_z + b^2 \\ &= (\hat{L}_z + Z_\alpha \sigma_r + Z_\eta \sigma_\phi)^2 - 2b\sigma_z \hat{L}_z + b^2, \end{aligned} \quad (\text{A3})$$

where $\{\sigma_z, \sigma_r\} = \{\sigma_z, \sigma_\phi\} = 0$ and $\sigma_z^2 = 1$ were used. Furthermore, we have

$$\begin{aligned} &(\hat{L}_z + Z_\alpha \sigma_r + Z_\eta \sigma_\phi)^2 \\ &= \hat{L}_z^2 + \{\hat{L}_z, Z_\alpha \sigma_r + Z_\eta \sigma_\phi\} + (Z_\alpha \sigma_r + Z_\eta \sigma_\phi)^2 \\ &= \hat{L}_z^2 + \{\hat{L}_z, Z_\alpha \sigma_r + Z_\eta \sigma_\phi\} + Z_\alpha^2 + Z_\eta^2 \\ &= \hat{L}_z^2 + [\hat{L}_z, Z_\alpha \sigma_r + Z_\eta \sigma_\phi] + 2(Z_\alpha \sigma_r + Z_\eta \sigma_\phi) \hat{L}_z \\ &\quad + (Z_\alpha^2 + Z_\eta^2), \end{aligned} \quad (\text{A4})$$

where we have used $\{\sigma_r, \sigma_\phi\} = 0$ and $\sigma_r^2 = \sigma_\phi^2 = 1$, and thus $(Z_\alpha \sigma_r + Z_\eta \sigma_\phi)^2 = Z_\alpha^2 + Z_\eta^2$. The irrelevant constants b^2 and $Z_\alpha^2 + Z_\eta^2$ that only shift the energy spectrum will be neglected. Therefore the operator \hat{D}_0^2 can be written as

$$\begin{aligned} \hat{D}_0^2 &= \hat{L}_z^2 + [\hat{L}_z, Z_\alpha \sigma_r + Z_\eta \sigma_\phi] \\ &\quad + 2(Z_\alpha \sigma_r + Z_\eta \sigma_\phi) \hat{L}_z - 2b\sigma_z \hat{L}_z \\ &\quad + \text{irrelevant constants}. \end{aligned} \quad (\text{A5})$$

In the following, we will show that Eq. (5) lead to Eq. (A1) with the equivalent form Eq. (A5) for the operator \hat{D}_0^2 . Equation (5) can be written as

$$H_{2D} = \frac{\mathbf{\Pi}^2}{2m} + H_\alpha + H_\eta + H_b + V(\mathbf{r}), \quad (\text{A6})$$

where $V(\mathbf{r}) = \frac{1}{2}k(r-R)^2$ and

$$\mathbf{\Pi} = \mathbf{p} - e\mathbf{A}, \quad \mathbf{A} = \left(-\frac{1}{2}yB, \frac{1}{2}xB, 0\right), \quad (\text{A7})$$

and

$$\begin{aligned} H_\alpha &= \alpha(\sigma_x \Pi_y - \sigma_y \Pi_x), \\ H_\eta &= \eta(\sigma_x \Pi_x + \sigma_y \Pi_y), \\ H_b &= g_1(y\Pi_x - x\Pi_y)\sigma_z + g_2(x^2 + y^2). \end{aligned} \quad (\text{A8})$$

The vector potential \mathbf{A} satisfies the Coulomb gauge $\nabla \cdot \mathbf{A} = 0$, and we have

$$\mathbf{\Pi}^2 = p^2 - 2e\mathbf{A} \cdot \mathbf{p} + e^2\mathbf{A}^2. \quad (\text{A9})$$

By using $\Phi = B\pi r^2$ and $\Phi_0 = h/|e|$, the second term of Eq. (A9) can be written as

$$\begin{aligned} 2e\mathbf{A} \cdot \mathbf{p} &= eB(xp_y - yp_x) \\ &= eB\hat{\ell}_z, \quad \hat{\ell}_z = -i\hbar \frac{\partial}{\partial \phi} \\ &= -2 \frac{\Phi}{\Phi_0} \frac{\hbar}{r^2} \hat{\ell}_z \\ &= -2 \frac{\hbar\gamma_0}{r^2} \hat{\ell}_z, \end{aligned} \quad (\text{A10})$$

where $\gamma_0 = \Phi/\Phi_0$, and the third term of Eq. (A9) becomes

$$e^2\mathbf{A}^2 = \gamma_0^2 \frac{\hbar^2}{r^2}, \quad (\text{A11})$$

where $x^2 + y^2 = r^2$ was used. On the other hand, based on the coordinate transformation $x = r \cos \phi$ and $y = r \sin \phi$, we have

$$\begin{aligned} \frac{\partial}{\partial x} &= \cos \phi \frac{\partial}{\partial r} - \frac{\sin \phi}{r} \frac{\partial}{\partial \phi}, \\ \frac{\partial}{\partial y} &= \sin \phi \frac{\partial}{\partial r} + \frac{\cos \phi}{r} \frac{\partial}{\partial \phi}, \end{aligned} \quad (\text{A12})$$

and thus, the operator p^2 becomes

$$\begin{aligned} p^2 &= -\hbar^2 \left(\frac{\partial^2}{\partial x^2} + \frac{\partial^2}{\partial y^2} \right) \\ &= -\hbar^2 \left(\frac{\partial^2}{\partial r^2} + \frac{1}{r} \frac{\partial}{\partial r} + \frac{1}{r^2} \frac{\partial^2}{\partial \phi^2} \right) \\ &= -\hbar^2 \left(\frac{\partial^2}{\partial r^2} + \frac{1}{r} \frac{\partial}{\partial r} \right) + \frac{1}{r^2} \hat{\ell}_z^2. \end{aligned} \quad (\text{A13})$$

Inserting Eqs. (A10), (A11), and (A13) into Eq. (A9), we obtain

$$\begin{aligned}\Pi^2 &= -\hbar^2 \left(\frac{\partial^2}{\partial r^2} + \frac{1}{r} \frac{\partial}{\partial r} \right) + \frac{1}{r^2} \hat{\ell}_z^2 + 2 \frac{\hbar \gamma_0}{r^2} \hat{\ell}_z + \gamma_0^2 \frac{\hbar^2}{r^2} \\ &= -\hbar^2 \left(\frac{\partial^2}{\partial r^2} + \frac{1}{r} \frac{\partial}{\partial r} \right) + \frac{\hbar^2}{r^2} \left(\frac{\hat{\ell}_z}{\hbar} + \gamma_0 \right)^2 \\ &= -\hbar^2 \left(\frac{\partial^2}{\partial r^2} + \frac{1}{r} \frac{\partial}{\partial r} \right) + \frac{\hbar^2}{r^2} \hat{L}_z^2.\end{aligned}\quad (\text{A14})$$

Furthermore, by using Eq. (A12), straightforward calculations lead to the results

$$\begin{aligned}\Pi_x &= (p_x - eA_x) = -i\hbar \cos \phi \frac{\partial}{\partial r} - \frac{\sin \phi}{r} \hbar \hat{L}_z, \\ \Pi_y &= (p_y - eA_y) = -i\hbar \sin \phi \frac{\partial}{\partial r} + \frac{\cos \phi}{r} \hbar \hat{L}_z.\end{aligned}\quad (\text{A15})$$

Substitute Eq. (A15) into Eq. (A8), and after straightforward calculations, we can obtain

$$\begin{aligned}H_\alpha &= \alpha \left(i\hbar \sigma_\phi \frac{\partial}{\partial r} + \sigma_r \frac{\hbar}{r} \hat{L}_z \right), \\ H_\eta &= \eta \left(-i\hbar \sigma_r \frac{\partial}{\partial r} + \sigma_\phi \frac{\hbar}{r} \hat{L}_z \right), \\ H_b &= -g_1 \hbar \hat{L}_z \sigma_z + g_2 r^2.\end{aligned}\quad (\text{A16})$$

Define the Hamiltonian \mathcal{H}_0 as

$$\mathcal{H}_0 = -\frac{\hbar^2}{2m} \left(\frac{\partial^2}{\partial r^2} + \frac{1}{r} \frac{\partial}{\partial r} \right) + \frac{1}{2} k(r-R)^2, \quad (\text{A17})$$

and insert Eqs. (A14), (A16), and (A17) into Eq. (A6), we have

$$\begin{aligned}H_{2D} &= \mathcal{H}_0 + \frac{\hbar^2}{2mr^2} \hat{L}_z^2 + \alpha \left(i\hbar \sigma_\phi \frac{\partial}{\partial r} + \sigma_r \frac{\hbar}{r} \hat{L}_z \right) + \eta \left(-i\hbar \sigma_r \frac{\partial}{\partial r} + \sigma_\phi \frac{\hbar}{r} \hat{L}_z \right) - g_1 \hbar \hat{L}_z \sigma_z + g_2 r^2 \\ &= \mathcal{H}_0 + \frac{\hbar^2}{2mr^2} \hat{L}_z^2 + i\hbar (\alpha \sigma_\phi - \eta \sigma_r) \frac{\partial}{\partial r} + \left(\frac{\alpha \hbar}{r} \sigma_r \hat{L}_z + \frac{\eta \hbar}{r} \sigma_\phi \hat{L}_z \right) - g_1 \hbar \sigma_z \hat{L}_z + g_2 r^2 \\ &= \mathcal{H}_0 + \frac{\hbar^2}{2mr^2} \hat{L}_z^2 - \hbar [\hat{L}_z, \alpha \sigma_r + \eta \sigma_\phi] \frac{\partial}{\partial r} + (\alpha \sigma_r + \eta \sigma_\phi) \frac{\hbar}{r} \hat{L}_z - g_1 \hbar \sigma_z \hat{L}_z + g_2 r^2, \\ &= \mathcal{H}_0 + \frac{\hbar^2}{2mr^2} \left\{ \hat{L}_z^2 - \left[\hat{L}_z, \frac{2m\alpha r^2}{\hbar} \sigma_r + \frac{2m\eta r^2}{\hbar} \sigma_\phi \right] \frac{\partial}{\partial r} + \left(\frac{2m\alpha r}{\hbar} \sigma_r + \frac{2m\eta r}{\hbar} \sigma_\phi \right) \hat{L}_z - \frac{2mg_1 r^2}{\hbar} \sigma_z \hat{L}_z \right\} + g_2 r^2,\end{aligned}\quad (\text{A18})$$

where in the third equality we have used the results $[-i\hbar \frac{\partial}{\partial \phi}, \sigma_r] = -i\hbar \sigma_\phi$ and $[-i\hbar \frac{\partial}{\partial \phi}, \sigma_\phi] = i\hbar \sigma_r$, which can be written as $\sigma_\phi = i[\hat{L}_z, \sigma_r]$ and $\sigma_r = -i[\hat{L}_z, \sigma_\phi]$. We also stress that in the presence of only Rashba coupling ($\eta = 0$ and $b = 0$) the second equality of Eq. (A18) is exactly the same with the result given in Ref. [26].³ Follow the procedure shown in Ref. [26], the term \mathcal{H}_0 is the unperturbed Hamiltonian, and its lowest energy eigenstate is

$$R_0(r) = \sqrt{\frac{N}{R\sqrt{\pi}}} e^{-(1/2)N^2(r-R)^2}, \quad N = \frac{mk}{\hbar^2}, \quad (\text{A19})$$

which leads to the result [26]

$$\left\langle \frac{\partial}{\partial r} \right\rangle = \langle R_0(r) | \frac{\partial}{\partial r} | R_0(r) \rangle = -\frac{1}{2R}. \quad (\text{A20})$$

Therefore the expectation value of H_{2D} with respect to the eigenstate Eq. (A19) is given by

$$\begin{aligned}\langle H_{2D} \rangle &= \frac{\hbar^2}{2mR^2} \left\{ \hat{L}_z^2 + \left[\hat{L}_z, \frac{m\alpha R}{\hbar} \sigma_r + \frac{m\eta R}{\hbar} \sigma_\phi \right] + 2 \left(\frac{m\alpha R}{\hbar} \sigma_r + \frac{m\eta R}{\hbar} \sigma_\phi \right) \hat{L}_z - \frac{2mg_1 R^2}{\hbar} \sigma_z \hat{L}_z \right\} + \langle \mathcal{H}_0 \rangle + g_2 R^2 \\ &= \frac{\hbar^2}{2mR^2} \left\{ \hat{L}_z^2 + [\hat{L}_z, Z_\alpha \sigma_r + Z_\eta \sigma_\phi] + 2(Z_\alpha \sigma_r + Z_\eta \sigma_\phi) \hat{L}_z - 2b \sigma_z \hat{L}_z \right\} + \langle \mathcal{H}_0 \rangle + g_2 R^2 \\ &= \epsilon \hat{D}_0^2 - \frac{\hbar^2}{2mR^2} (b^2 + Z_\alpha^2 + Z_\eta^2) + \langle \mathcal{H}_0 \rangle + g_2 R^2,\end{aligned}\quad (\text{A21})$$

where we have used Eq. (A5). Equation (A21) is obtained by integrating the radial part (r) only. Thus the differential operator with respect to the azimuthal angle and the spin operators are still present in the equation. The terms $-\frac{\hbar^2}{2mR^2} (b^2 + Z_\alpha^2 + Z_\eta^2) + \langle \mathcal{H}_0 \rangle + g_2 R^2$ is a irrelevant term that only shifts the energy spectrum and can be neglected. As a result, the Hamiltonian of the quantum ring is Eq. (A21) by neglecting those irrelevant terms. In this sense, we obtain Eq. (A1), namely, Eqs. (8) and (9).

³There is an overall minus sign for the definition of \hat{L}_z in comparison with Ref. [26], which is due to the use of the charge of electron, $e = -|e|$. In our paper, the quantum flux is $\Phi_0 = h/|e|$, and in Ref. [26], the quantum flux is $\Phi_0 = h/e$.

APPENDIX B: ANGULAR MOMENTUM OPERATOR

In this Appendix, we will show that the total angular momentum $\hat{J}_z = \hat{\ell}_z + \frac{\hbar}{2}\sigma_z$ commutes with $\hat{H}_0 = \epsilon\hat{D}_0^2$, where

$$\hat{D}_0 = \frac{\hat{\ell}_z}{\hbar} + \gamma_0 + Z_\alpha\sigma_r + Z_\eta\sigma_\phi - b\sigma_z. \quad (\text{B1})$$

Because the commutator $[\hat{J}_z, \hat{H}_0]$ can be written as $[\hat{J}_z, \hat{H}_0] = \epsilon\hat{D}_0[\hat{J}_z, \hat{D}_0] + \epsilon[\hat{J}_z, \hat{D}_0]\hat{D}_0$, we will show that $[\hat{J}_z, \hat{D}_0] = 0$. Firstly, we have

$$\begin{aligned} & \left[\frac{\hat{\ell}_z}{\hbar} + \frac{1}{2}\sigma_z, \hat{D}_0 \right] \\ &= \left[\frac{\hat{\ell}_z}{\hbar} + \frac{1}{2}\sigma_z, \frac{\hat{\ell}_z}{\hbar} + Z_\alpha\sigma_r + Z_\eta\sigma_\phi - b\sigma_z \right] \\ &= Z_\alpha \left[\frac{\hat{\ell}_z}{\hbar}, \sigma_r \right] + Z_\eta \left[\frac{\hat{\ell}_z}{\hbar}, \sigma_\phi \right] + \frac{1}{2}(Z_\alpha[\sigma_z, \sigma_r] + Z_\eta[\sigma_z, \sigma_\phi]). \end{aligned} \quad (\text{B2})$$

The first term of the second equality of Eq. (B2) can be written as

$$\left[\frac{\hat{\ell}_z}{\hbar}, \sigma_r \right] = \left[-i\frac{\partial}{\partial\phi}, \sigma_r \right] = -i\sigma_\phi. \quad (\text{B3})$$

Furthermore, we have

$$\left[\frac{\hat{\ell}_z}{\hbar}, \sigma_\phi \right] = \left[-i\frac{\partial}{\partial\phi}, \sigma_\phi \right] = i\sigma_r. \quad (\text{B4})$$

Using commutators in Eqs. (7) together with Eqs. (B3) and (B4), then Eq. (B2) becomes

$$\begin{aligned} & \left[\frac{\hat{\ell}_z}{\hbar} + \frac{1}{2}\sigma_z, \hat{D}_0 \right] \\ &= Z_\alpha(-i\sigma_\phi) + Z_\eta(i\sigma_r) + \frac{1}{2}[Z_\alpha(2i\sigma_\phi) + Z_\eta(-2i\sigma_r)] \\ &= 0. \end{aligned} \quad (\text{B5})$$

Therefore we have

$$\left[\hat{\ell}_z + \frac{\hbar}{2}\sigma_z, \hat{H}_0 \right] = 0. \quad (\text{B6})$$

Namely, the total angular momentum is conserved. The corresponding quantum number j_z^σ must be included in the energy eigenvalues and eigenvectors.

APPENDIX C: ENERGY EIGENVECTORS AND EIGENVALUES

In this Appendix, we will show that the eigenvectors of the Hamiltonian Eq. (8) are given by Eqs. (21) and (22) with eigenvalues given in Eq. (27). Consider the Hamiltonian [Eqs. (8)]

$$\hat{H}_0 = \epsilon\hat{D}_0^2, \quad (\text{C1})$$

where ϵ is a constant and the operator \hat{D}_0 [Eq. (9)] is given by

$$\hat{D}_0 = -i\frac{\partial}{\partial\phi} + \gamma_0 + Z_\alpha\sigma_r + Z_\eta\sigma_\phi - b\sigma_z. \quad (\text{C2})$$

For the convenience of derivations, we neglect the irrelevant normalized constant $1/\sqrt{2\pi}$. One of eigenvectors $\psi_\uparrow(\phi)$ can be written as

$$\begin{aligned} |\psi_\uparrow(\phi)\rangle &= e^{ij_z^\uparrow\phi} \left(\cos\frac{\xi}{2}e^{-i\phi/2}|\uparrow\rangle + \sin\frac{\xi}{2}e^{i\theta}e^{i\phi/2}|\downarrow\rangle \right) \\ &= \cos\frac{\xi}{2}e^{i(j_z^\uparrow-1/2)\phi}|\uparrow\rangle + \sin\frac{\xi}{2}e^{i\theta}e^{i(j_z^\uparrow+1/2)\phi}|\downarrow\rangle, \end{aligned} \quad (\text{C3})$$

where $|\uparrow\rangle$ and $|\downarrow\rangle$ are eigenvectors of σ_z [see also Eq. (18)], i.e., $\sigma_z|\uparrow\rangle = |\uparrow\rangle$ and $\sigma_z|\downarrow\rangle = -|\downarrow\rangle$. It follows that

$$\begin{aligned} \sigma_x|\uparrow\rangle &= |\downarrow\rangle, \quad \sigma_x|\downarrow\rangle = |\uparrow\rangle, \\ \sigma_y|\uparrow\rangle &= i|\downarrow\rangle, \quad \sigma_y|\downarrow\rangle = (-i)|\uparrow\rangle. \end{aligned} \quad (\text{C4})$$

This implies that

$$\begin{aligned} \sigma_r|\uparrow\rangle &= e^{i\phi}|\downarrow\rangle, \quad \sigma_r|\downarrow\rangle = e^{-i\phi}|\uparrow\rangle, \\ \sigma_\phi|\uparrow\rangle &= ie^{i\phi}|\downarrow\rangle, \quad \sigma_\phi|\downarrow\rangle = (-i)e^{-i\phi}|\uparrow\rangle. \end{aligned} \quad (\text{C5})$$

Use Eqs. (C3), (C5), and (C2), after straightforward calculations, we have

$$\begin{aligned} (\hat{D}_0 - \gamma_0)|\psi_\uparrow(\phi)\rangle &= C_\uparrow \cos\frac{\xi}{2}e^{i(j_z^\uparrow-1/2)\phi}|\uparrow\rangle \\ &\quad + C_\downarrow \sin\frac{\xi}{2}e^{i(j_z^\uparrow+1/2)\phi}e^{i\theta}|\downarrow\rangle, \end{aligned} \quad (\text{C6})$$

where $Z_\alpha + iZ_\eta = |Z|e^{i\theta}$ was used [see Eq. (25)], and the coefficients C_\uparrow and C_\downarrow are given by

$$\begin{aligned} C_\uparrow &= j_z^\uparrow - \frac{1}{2} - b + |Z|\tan\frac{\xi}{2}, \\ C_\downarrow &= j_z^\uparrow + \frac{1}{2} + b + |Z|\frac{1}{\tan\frac{\xi}{2}}. \end{aligned} \quad (\text{C7})$$

Furthermore, use Eq. (26), we have

$$\begin{aligned} C_\uparrow &= j_z^\uparrow - \frac{1}{2} - b + |Z|\tan\frac{\xi}{2} \\ &= j_z^\uparrow - \frac{1}{2} - b + |Z|\left(\frac{b+1/2}{|Z|} - \frac{\sqrt{|Z|^2 + (b+1/2)^2}}{|Z|} \right) \\ &= j_z^\uparrow - \sqrt{|Z|^2 + (b+1/2)^2}. \end{aligned} \quad (\text{C8})$$

For C_\downarrow , we have

$$\begin{aligned}
 C_\uparrow &= j_z^\uparrow + \frac{1}{2} + b + |Z| \frac{1}{\tan \frac{\xi}{2}} \\
 &= j_z^\uparrow + \frac{1}{2} + b + |Z| \left(\frac{|Z|}{(b+1/2) - \sqrt{|Z|^2 + (b+1/2)^2}} \right) \\
 &= j_z^\uparrow + \frac{1}{2} + b \\
 &\quad + |Z|^2 [(b+1/2) + \sqrt{|Z|^2 + (b+1/2)^2}] \frac{1}{-|Z|^2} \\
 &= j_z^\uparrow + \frac{1}{2} + b - [(b+1/2) + \sqrt{|Z|^2 + (b+1/2)^2}] \\
 &= j_z^\uparrow - \sqrt{|Z|^2 + (b+1/2)^2}.
 \end{aligned} \tag{C9}$$

We have to stress that up to this step we did not impose any constraint on the value j_z^\uparrow . Therefore we have

$$\widehat{D}_0 |\psi_\uparrow(\phi)\rangle = \left(\gamma_0 + j_z^\uparrow - \sqrt{|Z|^2 + \left(b + \frac{1}{2}\right)^2} \right) |\psi_\uparrow(\phi)\rangle. \tag{C10}$$

For the other eigenstate, we have

$$\begin{aligned}
 |\psi_\downarrow(\phi)\rangle &= e^{i j_z^\downarrow \phi} \left(-\sin \frac{\xi}{2} e^{-i\phi/2} |\uparrow\rangle + \cos \frac{\xi}{2} e^{i\theta} e^{i\phi/2} |\downarrow\rangle \right) \\
 &= -\sin \frac{\xi}{2} e^{i(j_z^\downarrow - 1/2)\phi} |\uparrow\rangle + \cos \frac{\xi}{2} e^{i\theta} e^{i(j_z^\downarrow + 1/2)\phi} |\downarrow\rangle.
 \end{aligned} \tag{C11}$$

Using Eqs. (C2), (C5), and (C11) and after straightforward calculations, we have

$$\begin{aligned}
 (\widehat{D}_0 - \gamma_0) |\psi_\uparrow(\phi)\rangle &= C'_\uparrow \left(-\sin \frac{\xi}{2} \right) e^{i(j_z^\downarrow - 1/2)\phi} |\uparrow\rangle \\
 &\quad + C'_\downarrow \cos \frac{\xi}{2} e^{i(j_z^\downarrow + 1/2)\phi} e^{i\theta} |\downarrow\rangle,
 \end{aligned} \tag{C12}$$

where $Z_\alpha + iZ_\eta = |Z|e^{i\theta}$ was used [see Eq. (25)], and the coefficients C'_\uparrow and C'_\downarrow are given by

$$\begin{aligned}
 C'_\uparrow &= j_z^\uparrow - \frac{1}{2} - b - |Z| \frac{1}{\tan \frac{\xi}{2}}, \\
 C'_\downarrow &= j_z^\uparrow + \frac{1}{2} + b - |Z| \tan \frac{\xi}{2}.
 \end{aligned} \tag{C13}$$

By using Eq. (26), we have

$$\begin{aligned}
 C'_\uparrow &= j_z^\downarrow - \frac{1}{2} - b - |Z| \left(\frac{|Z|}{(b+1/2) - \sqrt{|Z|^2 + (b+1/2)^2}} \right) \\
 &= j_z^\downarrow - \frac{1}{2} - b - |Z|^2 \frac{(b+1/2) + \sqrt{|Z|^2 + (b+1/2)^2}}{-|Z|^2} \\
 &= j_z^\downarrow - \frac{1}{2} - b + \left(b + \frac{1}{2}\right) + \sqrt{|Z|^2 + (b+1/2)^2} \\
 &= j_z^\downarrow + \sqrt{|Z|^2 + (b+1/2)^2}.
 \end{aligned} \tag{C14}$$

For C'_\downarrow , we have

$$\begin{aligned}
 C'_\downarrow &= j_z^\downarrow + \frac{1}{2} + b - |Z| \tan \frac{\xi}{2} \\
 &= j_z^\downarrow + \frac{1}{2} + b - |Z| \left(\frac{(b+1/2) - \sqrt{|Z|^2 + (b+1/2)^2}}{|Z|} \right) \\
 &= j_z^\downarrow + \frac{1}{2} + b - \left(b + \frac{1}{2}\right) + \sqrt{|Z|^2 + (b+1/2)^2} \\
 &= j_z^\downarrow + \sqrt{|Z|^2 + (b+1/2)^2}.
 \end{aligned} \tag{C15}$$

Therefore we obtain

$$\widehat{D}_0 |\psi_\downarrow(\phi)\rangle = (\gamma_0 + j_z^\downarrow + \sqrt{|Z|^2 + (b+1/2)^2}) |\psi_\downarrow(\phi)\rangle. \tag{C16}$$

We also stress that up to this step we didn't impose any constraint on the value j_z^\downarrow . Equations (C10) and (C16) give us the result

$$\begin{aligned}
 \hat{H}_0 |\psi_\sigma(\phi)\rangle &= \epsilon \widehat{D}_0^2 |\psi_\sigma(\phi)\rangle \\
 &= \epsilon \left(\gamma_0 + j_z^\sigma - \sigma \sqrt{|Z|^2 + \left(b + \frac{1}{2}\right)^2} \right)^2 |\psi_\sigma(\phi)\rangle,
 \end{aligned} \tag{C17}$$

where $\sigma = \uparrow, \downarrow$ and \uparrow indicates plus sign $+$; \downarrow indicates minus sign $-$ for the term $\sigma \sqrt{|Z|^2 + (b+1/2)^2}$. Importantly, hamiltonian \hat{H}_0 cannot directly determine the value j_z^\uparrow and j_z^\downarrow . This quantum number must be determined by using another conserved operator. We find that $\hat{J}_z = \hat{\ell}_z + \frac{\hbar}{2} \sigma_z$ commute with \hat{H}_0 , and the quantum number j_z^σ can be uniquely determined, as shown in Sec. II.

[1] M. V. Berry, *Proc. R. Soc. London A* **392**, 45 (1984).

[2] A. Tomita and R. Y. Chiao, *Phys. Rev. Lett.* **57**, 937 (1986); P. J. Leek *et al.*, *Science* **318**, 1889 (2007) and references therein.

[3] A. Bohm, A. Mostafazadeh, H. Koizumi, Q. Niu, and J. Zwanziger, *The Geometric Phase in Quantum Systems* (Springer, New York, 2003).

[4] P. Gentile, M. Cuoco, O. M. Volkov, Z.-J. Ying, I. J. Vera-Marun, D. Makarov, and C. Ortix, *Nat. Electron.* **5**, 551 (2022).

[5] G. Dresselhaus, *Phys. Rev.* **100**, 580 (1955).

[6] E. I. Rashba, *Sov. Phys. Solid State* **2**, 1109 (1960); Y. A. Bychkov and E. I. Rashba, *J. Phys. C* **17**, 6039 (1984).

[7] I. Žutić, J. Fabian, and S. D. Sarma, *Rev. Mod. Phys.* **76**, 323 (2004).

[8] J. Sinova, S. O. Valenzuela, J. Wunderlich, C. H. Back, and T. Jungwirth, *Rev. Mod. Phys.* **87**, 1213 (2015).

[9] D. D. Awschalom, D. Loss, and N. Samarth, *Semiconductor Spintronics and Quantum Computation*, 1st ed. (Springer, Heidelberg, 2002).

- [10] S. Datta and B. Das, *Appl. Phys. Lett.* **56**, 665 (1990); T. Koga, J. Nitta, H. Takayanagi, and S. Datta, *Phys. Rev. Lett.* **88**, 126601 (2002); J. C. Egues, G. Burkard, and D. Loss, *ibid.* **89**, 176401 (2002); M. Governale, *ibid.* **89**, 206802 (2002).
- [11] A. G. Aronov and Y. B. Lyanda-Geller, *Phys. Rev. Lett.* **70**, 343 (1993).
- [12] Y.-S. Yi, T.-Z. Qian, and Z.-B. Su, *Phys. Rev. B* **55**, 10631 (1997).
- [13] S.-L. Zhu, Y.-C. Zhou, and H.-Z. Li, *Phys. Rev. B* **52**, 7814 (1995); T.-Z. Qian, Y.-S. Yi, and Z.-B. Su, *ibid.* **55**, 4065 (1997).
- [14] J. Splettstoesser, M. Governale, and U. Zülicke, *Phys. Rev. B* **68**, 165341 (2003).
- [15] V. K. Kozin, I. V. Iorsh, O. V. Kibis, and I. A. Shelykh, *Phys. Rev. B* **97**, 155434 (2018).
- [16] A. F. Morpurgo, J. P. Heida, T. M. Klapwijk, B. J. van Wees, and G. Borghs, *Phys. Rev. Lett.* **80**, 1050 (1998); J.-B. Yau, E. P. De Poortere, and M. Shayegan, *ibid.* **88**, 146801 (2002).
- [17] M. Büttiker, Y. Imry, and R. Landauer, *Phys. Lett. A* **96**, 365 (1983); H. F. Cheung, Y. Gefen, E. K. Riedel, and W. H. Shih, *Phys. Rev. B* **37**, 6050 (1988).
- [18] T. Chakraborty and P. Pietiläinen, *Phys. Rev. B* **50**, 8460 (1994).
- [19] Y. V. Pershin and C. Piermarocchi, *Phys. Rev. B* **72**, 125348 (2005).
- [20] O. I. Pâtu and D. V. Averin, *Phys. Rev. Lett.* **128**, 096801 (2022).
- [21] L. P. Levy, G. Dolan, J. Dunsmuir, and H. Bouchiat, *Phys. Rev. Lett.* **64**, 2074 (1990); V. Chandrasekhar, R. A. Webb, M. J. Brady, M. B. Ketchen, W. J. Gallagher, and A. Kleinsasser, *ibid.* **67**, 3578 (1991); H. Bluhm, N. C. Koshnick, J. A. Bert, M. E. Huber, and K. A. Moler, *ibid.* **102**, 136802 (2009).
- [22] Y. Aharonov and D. Bohm, *Phys. Rev.* **115**, 485 (1959).
- [23] Y. Aharonov and A. Casher, *Phys. Rev. Lett.* **53**, 319 (1984).
- [24] A. Tonomura, N. Osakabe, T. Matsuda, T. Kawasaki, J. Endo, S. Yano, and H. Yamada, *Phys. Rev. Lett.* **56**, 792 (1986); M. König, A. Tschetschetkin, E. M. Hankiewicz, J. Sinova, V. Hock, V. Daumer, M. Schäfer, C. R. Becker, H. Buhmann, and L. W. Molenkamp, *ibid.* **96**, 076804 (2006).
- [25] J. Nitta, F. E. Meijer, and H. Takayanagi, *Appl. Phys. Lett.* **75**, 695 (1999).
- [26] F. E. Meijer, A. F. Morpurgo, and T. M. Klapwijk, *Phys. Rev. B* **66**, 033107 (2002).
- [27] H. Jensen and H. Koppe, *Ann. Phys.* **63**, 586 (1971); R. C. T. da Costa, *Phys. Rev. A* **23**, 1982 (1981).
- [28] Z. J. Ying, P. Gentile, C. Ortix, and M. Cuoco, *Phys. Rev. B* **94**, 081406(R) (2016); C. Ortix, *ibid.* **91**, 245412 (2015).
- [29] B. Molnár, F. M. Peeters, and P. Vasilopoulos, *Phys. Rev. B* **69**, 155335 (2004); U. Aeberhard, K. Wakabayashi, and M. Sgrist, *ibid.* **72**, 075328 (2005); S. Souma and B. K. Nikolić, *ibid.* **70**, 195346 (2004); M. Wang and K. Chang, *ibid.* **77**, 125330 (2008).
- [30] J. S. Sheng and K. Chang, *Phys. Rev. B* **74**, 235315 (2006).
- [31] A. A. Kovalev, M. F. Borunda, T. Jungwirth, L. W. Molenkamp, and J. Sinova, *Phys. Rev. B* **76**, 125307 (2007).
- [32] M. F. Borunda, X. Liu, A. A. Kovalev, X.-J. Liu, T. Jungwirth, and J. Sinova, *Phys. Rev. B* **78**, 245315 (2008); M. Pletyukhov and U. Zülicke, *ibid.* **77**, 193304 (2008); D. Stepanenko, M. Lee, G. Burkard, and D. Loss, *ibid.* **79**, 235301 (2009); M. Jääskeläinen and U. Zülicke, *ibid.* **81**, 155326 (2010).
- [33] B. A. Bernevig and S.-C. Zhang, *Phys. Rev. Lett.* **96**, 106802 (2006).
- [34] M. Z. Hasan and C. L. Kane, *Rev. Mod. Phys.* **82**, 3045 (2010) and references therein.
- [35] J. E. Moore, *Nature (London)* **464**, 194 (2010) and references therein.
- [36] L. Gioia, U. Zülicke, M. Governale, and R. Winkler, *Phys. Rev. B* **97**, 205421 (2018).
- [37] F. G. Medina, D. Martínez, Á. Díaz-Fernandez, F. Dominguez-Adame, L. Rosales, and P. A. Orellana, *Sci. Rep.* **12**, 1071 (2022).
- [38] In Ref. [28], the internal Zeeman field remains, and the electron spin acquires a finite out-of-plane component in the absence of spin-orbit interaction. The internal Zeeman field gives a nontrivial torque to the local spin. This consequence would be true in the system with nonconstant curvature as shown in Ref. [28], where the elliptical shape of ring is considered. The total angular momentum is not necessarily a constant of motion. However, for the circular ring (constant curvature) discussed in this paper, the total angular momentum is conserved.
- [39] D. Frustaglia and K. Richter, *Phys. Rev. B* **69**, 235310 (2004).
- [40] F. Nagasawa, D. Frustaglia, H. Saarikoski, K. Richter, and J. Nitta, *Nat. Commun.* **4**, 2526 (2013).
- [41] A. V. Balatsky and B. L. Altshuler, *Phys. Rev. Lett.* **70**, 1678 (1993).
- [42] S. Oh and C.-M. Ryu, *Phys. Rev. B* **51**, 13441 (1995).
- [43] P. M. Shmakov, A. P. Dmitriev, and V. Yu. Kachorovskii, *Phys. Rev. B* **85**, 075422 (2012).
- [44] M. Patra, *J. Phys.: Condens. Matter* **34**, 325301 (2022).